[Frontiers in Bioscience 14, 3188-3213, January 1, 2009]

Insight into the actin-myosin motor from x-ray diffraction on muscle

Sergey Y. Bershitsky[1], Michael A. Ferenczi[2], Natalia A. Koubassova[3], Andrey K. Tsaturyan[3]

[1]Institute of Immunology and Physiology, Russian Academy of Sciences, 91 Pervomayskaya ul. Yekaterinburg, 620041 Russia, [2]Molecular Medicine Section, National Heart and Lung Institute, Imperial College London, SW7 2AZ UK, [3]Institute of Mechanics, Moscow University, 1 Mitchurinsky prosp. Moscow, 119992 Russia

TABLE OF CONTENTS

1. ABSTRACT

The origin of reflections in the x-ray diffraction pattern from striated muscle and their use for understanding the structural organization of the contractile machinery are presented and discussed. Results of x-ray diffraction experiments obtained by a number of research groups using a variety of protocols revealed structural changes in contracting muscles which are interpreted in terms of molecular movements that underlie force generation. Some of these data are in line with the widely accepted 'lever arm' hypothesis which links force generation to a tilt of the light chain domain of the myosin head with respect to its motor domain. However, changes in the layer line intensities observed in response to various perturbations cannot be explained by tilting of the lever arm. Such changes, first revealed in response to temperature jumps, are interpreted as a transition of non-stereo-specifically attached myosin heads to a stereo-specifically bound state. The new 'roll and lock' model considers force-generation as a two-stage process: initial stereo-specific locking of myosin heads on actin is followed by the lever arm tilt.

2. INTRODUCTION

X-ray diffraction has provided the earliest information about the molecular structure of the contractile machinery in live muscle (1). The main advantage of this method is that it uniquely gives the possibility to obtain 3D structural information about contractile proteins in muscle or single muscle fibers whilst simultaneously monitoring their mechanical function. This structural information cannot be obtained from proteins in solution. The development of a new generation of synchrotron radiation sources and fast 2D x-ray detectors provides exciting possibility for studying structural changes in the actin-myosin motors in muscle with unique temporal (2) and spatial (3) resolution. Force in contracting muscle is produced by crossbridges, the globular heads of myosin molecules, which protrude from the thick filaments and cyclically interact with actin of the thin filaments. The interaction leads to a sliding of the two sets of filaments along each other i.e. to a shortening of sarcomere and/or to a force generation. The crossbridges are believed to act independently and asynchronously.

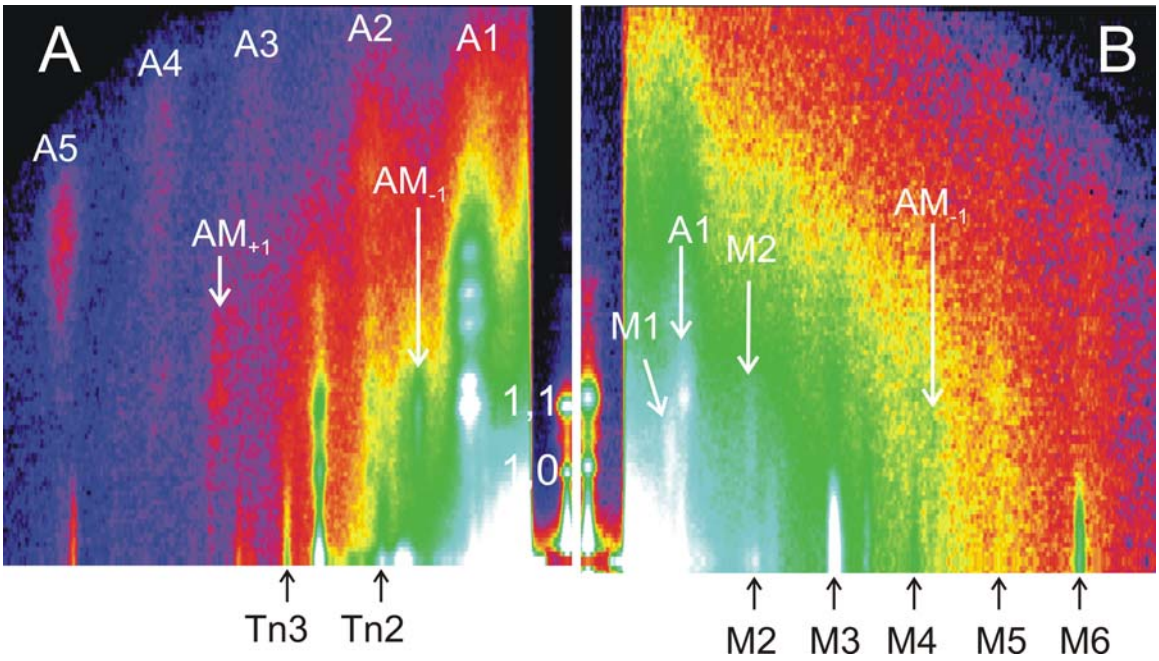

Figure 1. X-ray diffraction patterns collected from a single rabbit muscle fiber in rigor (A) and during active contraction at ~30 °C (B). Only one double-mirrored symmetric quadrant (0.155 nm^{-1}×0.155 nm^{-1} in reciprocal space) is shown for each pattern, the equator is vertical. Data collected from two ~3.5 mm long segments of a single muscle fiber; 400 ms exposure in each state; camera length 4.2 m; pseudo-color code and logarithm scaling intensity were used to visualize strong and weak x-ray reflections simultaneously. The equatorial, meridional and layer line reflections of interest are labeled. An attenuator strip was placed along the equator in front of a CCD detector to avoid its saturation; experimental methods were described earlier (9).

Synchronization of structural changes in a large population of myosin molecules in a muscle specimen can be achieved by fast perturbations of muscle length (4, 5), load (6), temperature (7, 8, 9), concentrations of ATP (10-15) or Ca^{2+} (16). These experimental approaches together with x-ray interferometry (3) and addition of exogenous proteins into muscle fibers (17-20) which had their cell membrane treated to make them permeable revealed new structural features of the actin-myosin molecular motor and of its regulation. The quantitative interpretation of x-ray diffraction data requires adequate mathematical modeling, based on the available high resolution structures of actin and of the myosin head as well as *a priori* information about the 3D organization of the thin and thick filaments in the sarcomere.

Several reviews of x-ray diffraction studies of muscle have been published recently (21-23) which mainly focused on changes in the intensity and fine structure of the myosin meridional reflections, principally the brightest one called M3. Here we discuss changes in all measurable reflections in the diffraction pattern, including layer lines, which are observed in the different experiments with vertebrate skeletal muscles. We believe that monitoring of changes in the entire diffraction pattern currently accessible, including those in the weak layer lines, is essential to give a comprehensive picture of structural events underlying the mechanism of the actin-myosin motor in muscle. Measurements of one or a few bright reflections do not provide sufficient information to derive complete understanding of molecular events underlying muscle contraction. Different factors affecting the intensities of the x-ray reflections are analyzed and discussed. Special attention is given to correlating of structural and mechanical changes as measured in time-resolved x-ray diffraction experiments.

3. X-RAY DIFFRACTION PATTERN FROM MUSCLE

Myofibrils in striated muscle form a well ordered system that consists of thin and thick filaments, which, when exposed to an x-ray beam, produces a whole set of equatorial, meridional and layer line reflections. Since the pioneering work of H.E. Huxley (1, 24, 25) these reflections provide information about muscle structure in different physiological and biochemical states which lead to understanding of the molecular movements which drive muscle contraction. The two-dimensional x-ray diffraction patterns from skeletal muscles in different states were described in detail and interpreted by Huxley and Brown (26).

The x-ray diffraction patterns from a single rabbit muscle fiber with a chemically permeabilized cell membrane in rigor (i.e. in the absence of ATP) and during isometric contraction at ~30 °C obtained on beamline ID02 at ESRF (Grenoble, France) are shown in Figure 1. The brightest reflections are seen in the equator, perpendicular to the filament axis. Reflections seen on the meridian, parallel to the fiber axis, are weaker. The layer line reflections parallel to the equator are generally even less intense than meridional ones.

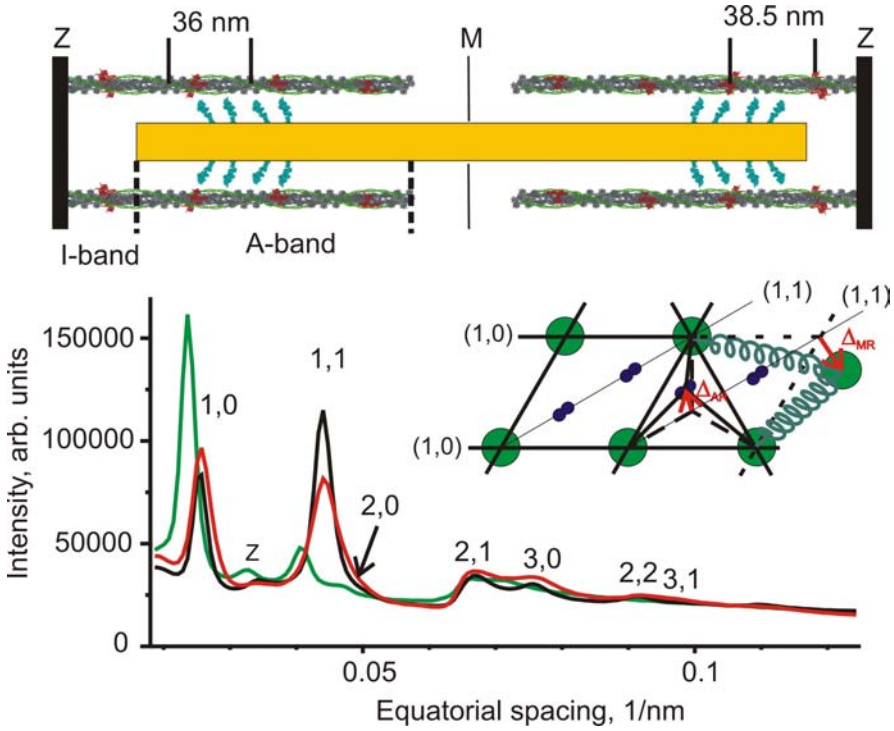

Figure 2. A diagram of the filament lattice in a sarcomere. Top: thin and thick filaments; Z-line, M-line, I-band and A-band are marked, actin monomers (gray), tropomyosin (green) and troponin (red), backbone of a myosin filament (yellow) and several myosin heads (cyan) are shown. The pitch or the cross-over repeat of the actin helix (36 nm) is different from the troponin axial repeat (38.5 nm) Inset: hexagonal filament lattice in the A-band of sarcomeres; the thick (green) and thin (blue) filaments, the (1,0) and (1,1) planes, and the deviations, Δ_{AR} and Δ_{MR}, of the actin and myosin filaments from ideal lattice positions for the disorder of the 1st and 2nd kind are shown. Bottom: equatorial profiles of x-ray diffraction intensity from a single permeabilized fiber from bony fish fin muscle in relaxed (green), rigor (black) states and during active contraction at ~5 °C (red) collected on ID02 at ESRF. The fiber was cross-linked with EDC as described (29); the x-ray exposure was 100 ms in each state, x-ray wavelength was 0.1 nm and the camera length was 2.5 m. A decrease in the intensities at spacing below ~0.064 nm^{-1} is caused by an attenuator strip placed in front of a CCD detector to shield it from the bright low angle 1,0 and 1,1 reflections and to avoid its saturation. The positions of several equatorial reflections are shown.

3.1. Equatorial reflections

In the myofilament overlap zone of the sarcomeres the thin and thick filaments form a hexagonal lattice where myosin filaments are in the lattice points and the thin filaments are in the trigonal points (Figure 2; ref. 27). This lattice produces a characteristic set of equatorial reflections. As the orientation of the filament lattice with respect to the incident x-ray beam is random, the diffraction pattern of a muscle or a single muscle fiber is the azimuthal average of the square of the Fourier transform of the electron density. Any equatorial reflection arises only from those parts of the sarcomere where the angle between the unit cell of the filament lattice and the beam is equal to the Bragg angle for this particular reflection. Formulas for the intensities and the spacing of different equatorial reflections can be found in ref. 28. Equatorial profiles of diffraction intensity collected from a fiber from fish fin muscle are plotted in Figure 2.

The two brightest equatorial reflections are termed the 1,0,0 and 1,1,0 (or simply 1,0 and 1,1) which correspond to diffraction from the two sets of planes shown in inset in Figure 2. The spacing of these reflections can be represented as $\sqrt{3}d/2$ and $d/2$, respectively, where d is the distance between neighboring thick filaments. The intensities, $I_{1,1}$, $I_{1,0}$, of these reflections change dramatically when relaxed muscle goes into rigor, a state in the absence of ATP where all myosin heads in the overlap zone bind actin (ref. 30; Figure 2). In rigor the intensity of the 1,1 reflection increases while that of 1,0 decreases compared to relaxed muscle. This derives directly from the movement of myosin heads that leave the vicinity of the backbone of the thick filaments to bind actin (30). During active contraction the ratio of the intensities of the 1,1 and 1,0 reflections is intermediate between those in the relaxed and rigor states (ref 31; Figure 2).

It has been suggested that the intensity ratio, $I_{1,1}/I_{1,0}$, provides an estimate of the fraction of myosin heads bound to actin during muscle contraction (31, 32). Evaluation of the fraction of actin-bound myosin heads based on this ratio is still used (33). However the equatorial intensities depend not only on the number of myosin heads bound to actin, but also on several other parameters. Firstly, these intensities depend on the degree of disorder of the filament lattice. In relaxed muscle the actin filaments

probably are not constrained to the trigonal lattice points by specific interactions with other sarcomere proteins but are 'boxed' into their positions by the three neighboring thick filaments. In rigor and during active contraction bound myosin heads from three surrounding myosin filaments are expected to hold a thin filament more strongly at the trigonal point. Therefore in the A-band of sarcomeres the disorder of the thin filaments is expected to be of the 1st kind, that is characterized by random uncorrelated deviations from ideal lattice points. For this kind of disorder the intensity of a reflection is proportional to the 'thermal' factor $\exp(-4\pi^2\Delta_{AR}^2R^2)$ where Δ_{AR} and R are the root mean squared deviation of an actin filament from the trigonal lattice point (see inset in Figure 2) and the spacing of the reflection in reciprocal space, respectively (34). The intensity distribution within a reflection in this case does not depend on Δ_{AR} and the whole reflection scales with the 'thermal' factor. Model calculations show that the only way to explain quantitatively the ratio of the 1,1 and 1,0 intensities in relaxed muscle is to assume a significant (up to 3 nm) value of Δ_{AR} (28), especially in the case of frog or fish muscles where the 1,1 intensity is particularly small (Figure 2). Otherwise the calculated $I_{1,1}$ is much higher than observed. This conclusion agrees well with electron microscopy data showing significant uncorrelated disorder of the thin filament on the transversal sections of quickly frozen relaxed rabbit muscle fibers especially at high temperature (35).

The thick filaments are held in the lattice points by M-line and possibly some other proteins which keep them together in the middle of the A-band and probably restrict their relative displacement in both axial and transverse directions (springs in in Figure 2). Such elastic neighbor-to-neighbor connections suggest that disorder of the thick filaments should be of the 2nd kind. For this kind of disorder a decrease in the intensity of the high order reflections is accompanied by an increase in their width (34). Indeed the width of the 1,1 reflection is somewhat higher than that of the 1,0 reflection and the higher order reflections are even wider (Figure 2). This observation demonstrates that filament disorder of the 2nd kind does indeed occur in muscle together with disorder of the 1st kind. This is difficult to measure the amount of disorder of each kind from experimental data. For this reason an estimate of the fraction of myosin heads attached to actin from observed equatorial intensities is also difficult. However several attempts were made to build the plain projection of the electron density of the filament lattice in different physiological states using Fourier synthesis of the equatorial reflections (36-38). The validity of the results depends not only on correct estimates for the filament disorder discussed above, but also on the correct attribution of phases to the equatorial reflection.

The arrangement of detached myosin heads around the thick filaments also has a strong influence on the equatorial intensities. It was found that in relaxed mammalian muscles an increase in temperature from ~5 °C to >20 °C induces a disorder-to-order transition that is accompanied by helical packing of initially disordered heads onto the backbone of the thick filaments (39). This transition is also accompanied by a decrease in the ratio of the 1,1 and 1,0 intensities (39, 40) and by an increased disorder of the thin filaments in the hexagonal filament lattice observed by electron microscopy (35).

It was also shown that the equatorial intensities are strongly affected by a small change in the lattice spacing so that even a small shrinkage or expansion of the lattice during a transition of muscle from one physiological state to another may be responsible for a large change in equatorial intensities (28). Depending on ionic strength, a significant, up to 10%, lattice shrinkage takes place when a permeabilized muscle fiber undergoes a transition from relaxed to rigor state (Figure 2). A slightly less pronounced further shrinkage occurs when fiber develops active force in the presence of ATP and Ca^{2+} (Figure 2). This is probably caused by the radial component of force produced by myosin heads when they bind to actin (41). Tetanic stimulation of intact muscle fibers under feed-back control of sarcomere length induced a ~2% lattice shrinkage, i.e. much smaller than induces by Ca^{2+} activation of permeabilized muscle fibers (42). In cardiac muscle, changes in the lattice spacing due to changes in sarcomere length and degree of activation are now discussed as a possible mechanism to explain 'Starling's law' of the heart (43, 44).

In the non-overlap zone of sarcomeres, i.e. in the I-band, the thin filaments do not follow hexagonal symmetry but rather tend to form a square lattice, characteristic of their incorporation into the Z-line (27). This square lattice produces an equatorial 'Z-reflection' in the diffraction pattern of muscle with a spacing in between the 1,0 and 1,1 reflections (Figure 2).

3.2. Meridional reflections

Meridional reflections on the diffraction pattern are due to periodic repeats of structural elements along the fiber axis. Meridional profiles of the x-ray diffraction intensity in the region of axial spacing from 0.012 to 0.42 nm^{-1} collected from bundles of three rabbit muscle fibers are shown in Figure 3.

3.2.1. Thin filament reflections

Meridional reflections which originate from the actin repeat with a spacing multiple of $(\sim 2.73\ nm)^{-1}$ correspond to the axial distance between neighboring actin monomers in the actin filament (Figure 2). We will call the first of these reflections A13 assuming that the actin helix has exactly 13 monomers per 6 turns, i.e. it is a 13/6 helix. Binding of myosin heads to actin in rigor (Figure 3*B*) or during active contraction (45-47) leads to a significant increase in the A13 intensity due to labeling of actin monomers by bound myosin heads which have a much higher diffracting power.

Small changes in the ~2.73 nm spacing of the A13 reflection were used for measuring axial extension of the thin filament due to applied load, Ca-activation or binding of rigor myosin heads in the absence of tension. Early experiments (45, 46) resulted in an estimate of the compliance of actin filaments of 0.2-0.3%/T_0,where T_0 is isometric tension.

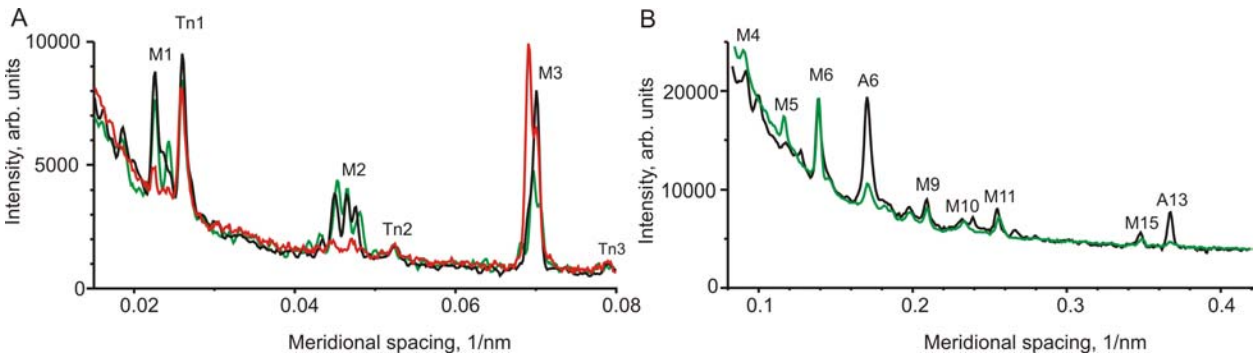

Figure 3. Meridional intensity profiles from bundles of three rabbit muscle fibers in relaxed (green) and low-tension rigor (black) states and during isometric contraction at ~30 °C (red). Data collected on ID02 at ESRF with camera of lengths of 10 m (A) and 2.5 m (B); the positions of some reflections are shown; other experimental details were described previously (9, 49).

Later it was found that activation itself induces a shortening of the actin filaments so that higher, up to $0.6\%/T_0$ estimates for elastic extension of the actin filaments were made (47, 48). More recently it was shown that the tight binding of myosin heads to actin itself induces up to a 0.2% elongation of the actin filaments in the absence of tension (49). In consequence, the low values for actin compliance obtained in mechanical experiments (50) are now compatible with the x-ray data.

Apart from the actin-based meridional reflections, the thin filaments produce a set of meridional reflections arising from regulatory protein troponin, with a spacing multiple of ~38.5 nm, 7-fold larger than that of the A13 actin reflection. Troponin is probably bound to every seventh actin monomer in a pseudo-two-strand actin helix (Figure 2) or, more precisely, to every 14th monomer in the actin helix (38.5 nm = 14×2.75 nm). Troponin-based reflections in the 2D diffraction patterns shown in Figure 1 and in the one-dimensional intensity profiles in Figure 3*A* are labeled Tn1, Tn2, and Tn3. The intensities of these reflections do not change much upon binding of rigor myosin heads to actin or during isometric contraction induced by Ca^{2+}-activation of troponin-C (Figure 3*A*).

3.2.2. Thick filament reflections

All other visible meridional reflections originate from the thick filaments. The most prominent are those with a spacing multiple to the ~43 nm pitch of the myosin helix when a muscle is in the relaxed state. They are called M1, M2 *etc* and have a spacing of 43 nm (M1), 21.5 nm = 43 nm/2 (M2), 14.33 = 43 nm/3 (M3) *etc* (Figure 3). In the case of a perfect three-strand helix where each of three crowns of three myosin molecules (and six heads respectively) per a pitch is rotated by 40° and shifted axially by ~14.33 nm with respect to its neighboring crowns (27) the meridional reflections observed should be only those with the indices multiple of 3: M3, M6, M9, *etc*. However there are other myosin meridional reflections, M1, M2, M4, M5 *etc.* called 'forbidden' which are caused by deviations from the perfect three-fold symmetry. The 'forbidden' reflections are very bright in relaxed muscles, slightly less intense in rigor and much weaker during contraction (Figure 3). The deviation from three-fold symmetry was attributed to the effect of C-protein on the structure of the thick filament (51, 52). C-protein (MyBP-C) is a myosin-binding protein that is usually seen as seven to nine stripes in each half of the A-band with a periodicity exactly or closely matching that of M1 (27).

The spacing of the myosin meridional reflection increases slightly when relaxed muscle goes into rigor (Figure 3*A*, *B*) and elongates further during isometric contraction at full activation (Figure 3*A*). The spacing of the brightest myosin reflection, M3, is 14.34 nm in relaxed frog muscle, 14.42 nm in rigor (26) and 14.56 nm during isometric contraction (53). Similar, up to ~1.5%, spacing changes upon development of isometric tetanus at full overlap were found in M6 and higher order myosin reflections (45, 46, 53-55). Such large extension of myosin filaments is probably caused not by their elasticity, but rather results from some structural changes in their backbones. The physical nature of these changes is unknown. The dependence of these changes on sarcomere length is rather complicated. When relaxed frog muscle was stretched from full-overlap to a non-overlap sarcomere length, the spacing of the high order myosin meridional reflections, M6, M9 and M15, increased by 0.4-0.8% (46). Electrical stimulation at non-overlap did not induce further changes in the spacing of these reflections, although at half-overlap ~1% elongation close to that at full overlap was observed (46). When muscles or single fibers contracting at full overlap were allowed to shorten under very low load, the spacing of the M3 (and M6) meridional reflection partially returned to its relaxed value (to 14.4-14.45 nm for the M3 reflection; 55, 56).

In contracting muscle the M3 intensity, I_{M3}, is believed to come from myosin heads, both attached and detached (5). A nearly linear decrease in I_{M3} with the decrease in length of the overlap zone between the thin and thick filaments at higher sarcomere length suggests that attached heads make a major contribution to the M3 intensity (58). Many authors believe that the M6 and higher order myosin meridional reflections originate mainly from structures on the myosin backbone so that the spacing changes of this reflection give a direct measurement of the myosin filament compliance (5, 6, 57). Others argue that all

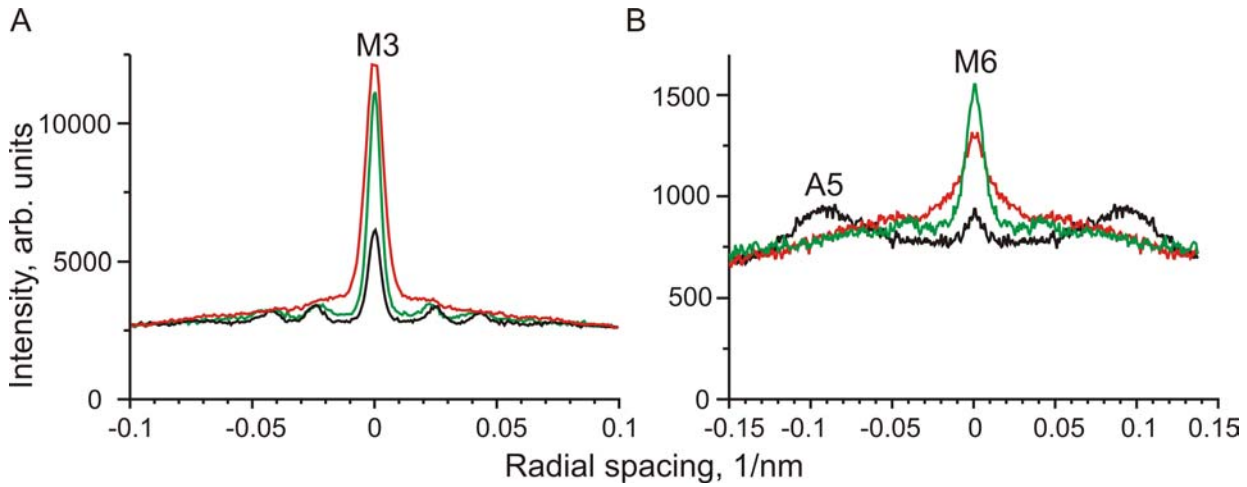

Figure 4. Radial intensity profiles of the M3 (A) and M6 (B) meridional reflection. Data from a single fiber from bony fish fin muscle in relaxed (green) and rigor (black) states and during active contraction at 5 °C (red). A: un-mirrored M3 profiles from one side of the patterns; B: M6 profiles after horizontal and vertical mirroring. Strong sampling of the 1,0 and 1,1 row lines is seen in the relaxed and rigor profiles of M3. Same data set as in Figure 2B. The off-meridional peaks on the M6 layer line in rigor are due to the contribution of the neighboring actin layer line A5 that has spacing close but not exactly equal to that of M6.

myosin meridional reflections in contracting muscle mainly originate from the heads (59, 60). An increase in the M6 intensity by up to 60% after step releases and its decrease by up to 25% after step stretches (57, 61) or during shortening at maximal velocity (56) show that a substantial part of the M6 intensity comes from attached myosin heads although another structure, probably the myosin backbone also contributes.

True elastic extensibility of the thick filaments was estimated by applying step length changes to contracting muscles or single fibers. Immediately at the end of 0.1 ms long step, the spacing of the M3 reflections in single intact muscle fibers increased by 0.14% per T_0 (3). By the end of the fast partial tension recovery following a length step, the increase in the M3 spacing was much larger, 0.34%/T_0 (3). A similar figure of 0.33-0.36%/T_0 was found for the delayed change in the M3 spacing in experiments with whole frog muscles (57).

A figure of 0.26%/T_0 for compliance of the myosin filaments was obtained from measurements of the spacing of the M6 meridional reflection in experiments with step changes in load (6, 57). It should be noted that changes in the spacing of myosin meridional reflections may originate from two different sources: (i) changes in the ~14.5 nm axial period of crown of myosin molecules along a thick filaments, and (ii) changes in length of the actin filaments. Actin elongation or shortening may affect the spacing of a myosin reflection if its intensity partially comes from the myosin heads attached to actin. The interpretation of the changes in the spacing of a myosin meridional reflection in terms of extensibility of the myosin filaments becomes even more difficult if attached myosin heads undergo some conformational changes after the length or load step. Estimates of the myosin filament compliance derived from the changes in spacing of M6 and higher order myosin reflections are probably more correct than those based on M3 although a contribution from bound myosin heads and therefore sensitivity to actin compliance cannot be eliminated.

During the onset of isometric tetani in intact frog muscle (5, 62) or single muscle fibers (55, 56) I_{M3} decreases and then increases again. This change in the intensity of the M3 meridional reflection is accompanied by an increase in its lateral spread (62, Figure 4). Huxley and co-authors have pointed that this spread, now it is more often called the radial width of the reflections, depends on the accuracy with which the lateral alignment of the thick filaments is maintained (62). In relaxed frog muscle the width of the M3 meridional reflection corresponds to a lateral size of coherently diffracting structure of 400 nm that is close to the radius of a myofibril (26). During contraction the width of the M3 meridional reflection increases nearly twice probably because active force induces axial disorder of neighbor thick filaments, i.e. decreases the size of the coherent unit (62; Figure 4*A*). To correct the observed integral intensity of a reflection for the effect of filament disorder it was suggested to multiply its measured value by the width at half maximum (62). After that, the corrected intensity increases significantly during the onset of isometric tetanus (62, 56). It was suggested that the axial disorder of the myosin filaments is 'disorder of the 2nd kind' so that the effect of axial registration/disorder of the thick filaments on the radial intensity distribution of a myosin meridional reflection can be expressed explicitly (63).

Since axial disorder of the myosin filaments leads to a decrease in the intensities of the meridional reflections, especially of M3 (and also of M6, Figure 4*A*, *B*), careful measurement of their width is necessary for correcting for the disorder. For example an increase in the temperature of contracting intact frog muscle fibers from 2 °C to 17 °C

leads to only a ~11% increase in the observed I_{M3} while after correction for the width, the intensity increases by ~30% (64). Similar figures for temperature-induced increases in I_{M3} were found in contracting permeabilized fibers from the frog where filament disorder was partially prevented by slight cross-linking with EDC (8). A more pronounced, ~60% increase in I_{M3} was observed in rabbit muscle fibers upon T-jumps from 5 °C to 30 °C (9). Temperature dependence of isometric tension is also steeper in rabbit muscle fibers than in the frog although the number of myosin heads attached to actin, as estimated from stiffness measurements, is temperature independent for both species (8, 65, 66). Speaking more general there is a strong correlation between the M3 intensity during isometric contraction and the level of average force produced by a crossbridge.

The width of meridional reflections in rigor depends crucially on the procedure by which muscle was put into rigor. If special precautions are taken to avoid development of high rigor force and to prevent filament disorder (29), the resting and rigor profiles of the M3 reflection have nearly the same width and are similarly sampled by the 1,0 and 1,1 row lines (Figure 4).

Change in the M3 intensity in contracting muscle in response to mechanical perturbations is often interpreted in terms of tilt of myosin heads (5, 67) or their light chain domains (2, 68-70). Such interpretation is correct only under conditions when no change in the population of myosin heads bound to actin takes place, i.e. no crossbridge detachment or attachment occurs. Otherwise changes in the number of attached myosin heads or in the dispersion of their positions from the 14.5 nm repeat strongly affect I_{M3} (63, 78). All four factors: the number of myosin heads bound to actin, their shape, the standard deviation of their axial positions from the 14.5 nm repeat, and axial misalignment of the neighboring myosin filaments are important determinants of the intensity of the M3 (and possibly other) myosin meridional reflections.

The fine axial structure of myosin meridional reflections is seen as bunches of closely positioned peaks within a reflection (see M3 in Figure 3*A*) and was observed in early experiments on whole muscle of the frog by H.E. Huxley and Brown (26).

The splitting of the meridional reflections is caused by interference between the x-rays diffracted by each of the two symmetrical halves of a sarcomere (71-74). Later Malinchik and Lednev (75) recorded high-resolution diffraction patterns from relaxed frog muscle and suggested a model that reproduced the main features of the pattern including the fine structure of meridional reflections and the myosin layer lines up to M6. Their model included C-protein stripes, a 'perturbed' region, i.e. deviation of axial positions of the crowns of myosin heads in the C-zone from their exact 14.3 nm periodicity, and a 3D model of a myosin head. This approach became the basis for further models of myosin-based x-ray reflections.

The development of new highly collimated and high flux x-ray sources made it possible to study the interference phenomenon in contracting muscle. X-ray diffraction patterns from single intact muscle fiber contracting at three different sarcomere lengths showed that the interference distance for the M3 reflection is exactly the center-to-center distance between the symmetrical arrays of attached myosin heads in two halves of a thick filament in a sarcomere (58). On the basis of these results the interferometry was suggested as a new tool for measuring sub-nanometer axial displacements of attached myosin heads during muscle contraction (3) and in rigor (76). The idea of the method is that any axial displacement of the crossbridges results in a change in the interference distance between the arrays and, respectively, in a change in the spatial frequency of the interference modulation (Figure 5).

Experimentally the change in frequency is seen as a shift in the positions and in the ratio of the intensities of the two main peaks of a reflection sampled by the interference function. A sub-nanometer displacement can be resolved by this method if the intensities of the peaks are measured with sufficiently high precision (Figure 5).

The fine structure of myosin meridional reflections up to M15 in isometrically contracting whole muscle was resolved by Juanhuix *et al.* (59). The authors estimated the contribution of C-protein and tropomyosin to the myosin meridional reflections and concluded that their impact at the plateau of an isometric tetanus is negligible, so that all myosin meridional reflections mainly originate from myosin heads. Their intensities were used for finding the configurations of myosin heads during active contraction. The analysis was based on a model accounting for the shape of the myosin heads from which their axial disposition can be determined. The authors found that the apparent interference distance (L in Figure 5 and legend) decreases with the order of the reflection. To fit this observation their model included a slight variation in the crown-to-crown distances. Using the model, a one-dimensional electron density map of a head crown was suggested.

A recent model (60) explains the interference splitting of all myosin meridional reflections up to M15 and the presence of the 'forbidden' reflections using defined assumptions about the size and properties of the 'perturbed' and 'not perturbed' regions on a myosin filament. The authors assumed that the size of the perturbed zone is different from the length of the C-zone and that it changes when muscle develops active tension. However these additional assumptions do not have so far any independent experimental support.

3.3. Layer lines

3.3.1. Myosin layer lines

Myosin layer lines have spacing multiple of ~1/43 nm^{-1} and originate from the myosin filaments. In relaxed skeletal muscles of the cold-blooded animals the intensities of all myosin layer lines are very high (26). In this state the heads of myosin molecules are packed in the vicinity of the backbone of the thick filaments at an average distance from the centre of the filament of <15 nm (26, 75, 77). In muscles of warm-blooded animals the myosin layer

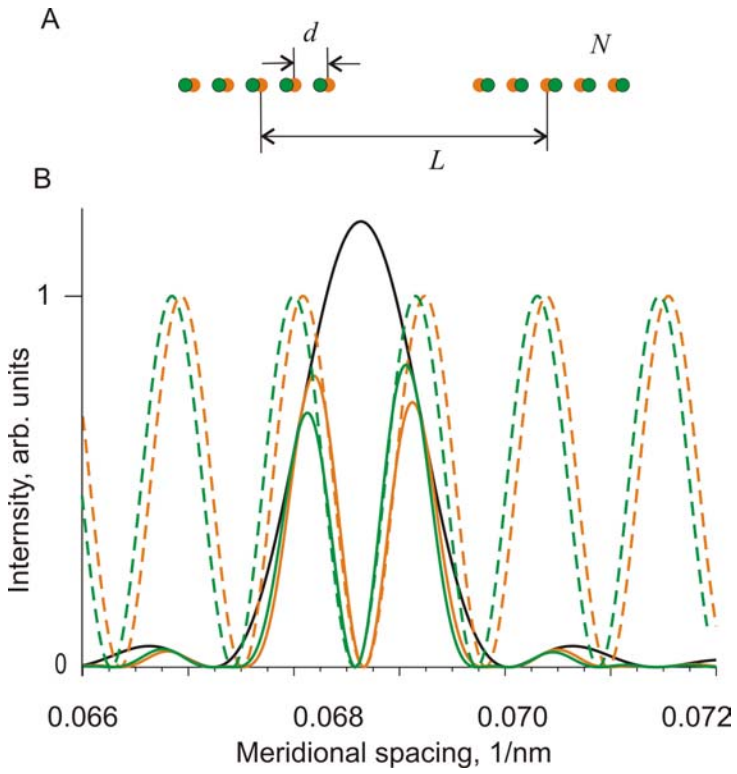

Figure 5. Scheme of x-ray diffraction interference of two symmetrical halves of a sarcomere. A: one-dimensional model of crossbridges in a sarcomere (M-line is the middle). $N = 49$ crowns of crossbridges (one attached myosin head or a pair of heads, where at least one head is attached to actin) separated by a distance d of ~14.5 nm are drawn as orange circles. L is the distance between the centers of the arrays or the interference distance. The intensity I at the spacing Z along the meridian can be calculated as the squared Fourier transform of the electron density of the two symmetrical arrays of myosin heads, $I(Z) = |F(Z)|^2 \cos^2(\pi LZ + \phi) \sin^2(\pi NdZ) / \sin^2(\pi dZ)$, where F, ϕ are the Fourier transform of the electron density of the 'average' crossbridge in a crown and its phase ($F = 1$, $\phi = 0$ in the case of the point diffractor model where the shape of crossbridges is not taken into account). Green circles correspond to crossbridges displaced by 0.5 nm towards the Z-line in each half of the sarcomere. B: x-ray intensity distribution (continuous orange and green lines, corresponding to two positions of crossbridges) calculated as the product of the diffracted intensity from an array of 49 point diffractors with $d = 14.57$ nm (black) and the interference function $\cos^2(\pi LZ)$, with $L = 866.56$ nm (orange dashed) and $L = 867.56$ nm (green dashed). The ratio of the peak intensities changes from 0.91 (orange) to 1.18 (green).

lines at low temperature (≤5 °C) are significantly less intense due to a disorder of the myosin heads. These intensities increase to a level characteristic for the cold-blooded animals upon increase in temperature to ≥20 °C (39, 79-81). The temperature-induced disorder-to-order transition of the thick filaments is associated with ATP hydrolysis (39, 81) or more precisely with a transition of myosin heads with bound ATP or ADP and P_i from 'open' to 'close' conformation (82). It appears that the heads in the closed state tend to bind their neighbors and the backbone of the thick filament to form a regular ordered structure while those in the open state are more disordered. An increase in temperature, the use of nucleotide-triphosphates other than ATP or of ATP analogs shifts the equilibrium between these two states (82, 83). Treatment of fibers with N-ethylmaleimide, that fixes S1 in the open state, leads to a reduction in the intensities of all myosin layer lines (84). In rigor where all myosin heads are strongly bound to actin (85) the off-meridional intensities of all myosin layer lines are much lower than in relaxed muscle although some myosin meridional reflections, including M2, M3 and M6, are quite bright (Figure 1; refs. 26, 54).

During active contraction the intensities of the 'forbidden' myosin meridional reflections M1, M2 and of the off-meridional myosin layer lines decrease dramatically compared to those in relaxed muscle (Figure 3; refs. 62, 54). When whole frog muscle contracts isometrically at low temperature the off-meridional M1 intensity is only ~15% of its relaxed value (54). An even lower M1 intensity was found in contracting single intact frog muscle fibers (55). When contracting muscle is allowed to shorten under very low load the M1 intensity is about three times higher than during isometric contraction although remains nearly half of that in the relaxed state (47). As the fraction of myosin heads bound to actin decreases when contracting muscle shortens at maximal velocity (86, 87), the data suggest that the myosin layer lines in contracting muscle mainly result from x-ray diffraction of the detached myosin heads.

On the other hand, there is evidence for a substantial contribution of weakly bound myosin heads with either ATP (88) or ADP·P_i (89) in their active sites to the off-meridional intensity of the myosin layer lines. To dissect the contribution of weakly bound heads from that of detached ones, x-ray diffraction patterns from muscle fibers with permeabilized cell membrane in the absence of Ca^{2+} were compared at different sarcomere length, temperature, ionic strength, in the absence and in the presence of polyethylene glycol that promotes weak binding. Modeling of x-ray diffraction patterns of muscles with weakly bound myosin heads was performed (90) to obtain a quantitative description of the experimental data (88). The modeling suggests that weak binding of myosin heads to actin with a ~70° full range of dispersion of axial attachment angles and a ~150° full range of dispersion of azimuthal attachment angles fits the intensity profiles for myosin layer lines from M1 to M6.

3.3.2. Actin layer lines

Actin layer lines have spacings multiple of ~1/36 nm^{-1} (Figures 1, 2). The presence of a meridional spot at about 2.73 nm, the bright layer lines at ~5.9 nm and ~5.1 nm which are clearly seen even in the resting state, and the first layer line at about 36 nm suggest the 13/6 helical model for the actin helix with 13 actin monomers per 6 helical turns (26). The 13/6 model is a rough approximation and more complicated models such as 67/31, 132/61 or 69/32 have also been suggested for different states of F-actin from high resolution x-ray diffraction on oriented gels of F-actin (91). Here we will use the simplest 13/6 nomenclature for the actin layer lines. A1 is the 1st actin layer line at ~(36 nm^{-1}), A6 and A7 are layer lines with spacings of ~(5.9 nm)$^{-1}$, and ~(5.1 nm)$^{-1}$, *etc*. Most probably F-actin is a non-integral helix and also not a precisely periodic structure. This agrees with observations showing that actin layer lines are intrinsically much wider than myosin layer lines (Figure 1). Several factors are known to affect the F-actin structure. Changes in the intensities of A1, A2 and A6 actin layer lines (92, 93) and in the axial shift and angle between two neighbor monomers (46, 47) of the actin helix occur upon activation of intact muscle under conditions when no crossbridge attachment takes place. Strong binding of myosin heads also stretches and twists the actin helix (49).

In relaxed muscle almost all actin layer lines are weak as myosin heads are located near the thick filaments and the actin layer lines are produced only by the thin filament proteins themselves. The bright layer lines are A6 and A7 at ~5.9 and ~5.1 nm, respectively, which have intensity peaks at a reciprocal radius of 0.07-0.09 nm^{-1} and A1 and A2 at higher (0.12-0.4 nm^{-1}) reciprocal radii. The A6 and A7 layer lines in relaxed muscle are mainly produced by actin while the high angle peaks on the A1 and A2 layer lines result from x-ray diffraction on both actin and tropomyosin (92, 93). Troponin also contributes to actin layer line intensities. Its contribution depends on activation of the thin filaments with Ca^{2+} and on strong binding of myosin heads to actin (158).

In rigor all actin layer lines become very intense because myosin heads strongly bind actin thus increasing the diffracting power of the actin helix (Figure 1; ref. 26). Rigor values of the intensities of the actin layer lines can be used as scaling factors for the intensities in other physiological or biochemical states of muscle as all myosin heads in rigor are strongly bound in rigor in vertebrate muscles. Further increase in the intensities of all actin layer lines can be achieved by addition of myosin heads (or S1) to permeabilized muscle fibers stretched to a sarcomere length of 3-4 μm where overlap between the thin and thick filaments is small or absent (17-20).

In rigor the intensity of the A6 actin layer line, I_{A6}, increases about twice compared to its relaxed value, mainly in the vicinity of the meridian, with a peak at a reciprocal spacing of 0.04-0.05 nm^{-1} (94, 95, 17). Addition of S1 to stretched muscle fibers to non-overlap leads to a further increase in I_{A6} at the same reciprocal radius. When short S1 constructs lacking the light chain domains (LCD) were added instead of a full length S1, the position of the A6 peak was slightly shifted to higher reciprocal radius (17). However even after addition of truncated S1 the position of the A6 peak was at much lower reciprocal radius than in relaxed muscle. These data demonstrate that LCDs of strongly bound myosin heads mainly contribute to the near-meridional A6 intensity (*ibid.*). Titration of muscle fibers with ATP-γS that detaches rigor myosin heads from actin also showed that rigor myosin heads mainly affect the intensity of this layer line at a reciprocal radius of ~0.05 nm^{-1} (95, 17). The intensity I_{A7} of the A7 actin layer line also increases by a factor of ~2 upon binding of myosin heads in rigor although the position of the intensity peak on this layer line does not change much compared to relaxed state (94).

Very small changes in the intensity profiles of the actin layer lines were observed upon ADP binding to muscle fibers with permeabilized membrane which were stretched to non-overlap and decorated with fast skeletal S1. More pronounced changes were found when slow skeletal/cardiac myosin S1 and especially S1 from smooth muscle or non-muscle myosin II were soaked into fibers in the same conditions (20). The changes in the layer line intensities were used for inferring a picture of the ADP-induced conformational changes in different strongly bound actin-S1 complexes.

While nucleotide-free S1 or S1·ADP complex bind actin strongly, S1 complexes with ATP or ADP and P_i have much lower affinity for actin (96). The effect of weak binding of myosin heads to actin on the intensities of the actin layer lines is not well understood. An increase in the A1 layer line intensity, I_{A1}, was shown to occur upon a decrease in the ionic strength of the relaxing solution bathing permeabilized muscle fibers treated with N-phenylmaleimide (88). The treatment stops ATP hydrolysis and leaves myosin heads in a state where only weak binding to actin is possible while low salt was shown to promote weak binding (97, 98). On the other hand no increase in I_{A6} upon weak binding was found in experiments (88), suggesting that weak binding to actin is non-stereo-specific (99, 88, 90). Such binding is characterized by a range of azimuthal and axial angles of attachment of myosin heads to actin. As the weak binding

is very sensitive to the ionic strength (98) it is probably mainly electrostatic.

The dispersion of the attachment angles results in a significantly lower contribution of the non-stereo-specifically attached myosin heads to actin layer lines than that of strongly, stereo-specifically bound ones. Diffraction theory suggests that dispersion of axial attachment angles mainly affect the intensities of the high-order actin layer lines, while the azimuthal dispersion primary depresses those layer lines where the intensity depends on the contribution of the Bessel functions of higher orders (34, 63, 78). This means that the dispersion of axial attachment angles is expected to depress the A5, A6 and A7 intensity more significantly than that of A1 and A2. On the other hand, dispersion of the azimuthal attachment angle should marginally decrease I_{A6} and I_{A7} because the main Bessel term for these layer lines is J_1. The A1 layer line with the main Bessel terms J_2, and especially A2, A3, A4 where J_4 and higher order Bessel functions dominate are expected to be much more sensitive to the azimuthal disorder than A6 and A7. The effect of the non-stereo-specifically bound myosin heads on the actin layer line intensities was estimated using S1 covalently cross-linked to actin with a zero-length linker, EDC, in overstretched muscle fibers (18). When uncross-linked S1 was washed out, addition and washing out of ATP induced reversible changes in the intensities of all actin layer lines. These intensities in the presence of ATP were indistinguishable from those recorded from the same muscle specimens in relaxing solution before addition of S1 and EDC treatment. This means that despite the covalent link between actin N-terminal and S1 loop 2 the amount of axial and azimuthal disorder of these heads is so high that they do not contribute to the actin layer lines.

An increase in I_{A6} during development of isometric contraction of intact frog muscle was found a long time ago (100). The increase in I_{A6} in contracting muscle compared to the relaxed state is about 30-40% of that in rigor muscle (17). However the position of the peak of the A6 layer line is not shifted towards the meridian as in rigor, but remains at about the same reciprocal radius as it is in relaxed muscles (94, 17). On the other hand, a small shift of the A6 peak towards the meridian can be seen during isometric contraction at higher temperature when muscle tension increases significantly (9). An increase in I_{A7} during development of isometric contraction is even more pronounced than that of I_{A6}, up to 60% of its increase upon the transition from relaxed to rigor states. The position of the A7 peak in relaxed and rigor states and in contracting muscle remains at about the same reciprocal radius (0.075-0.09 nm^{-1}; 94, 17). An increase in I_{A6} and I_{A7} in contracting muscle with temperature was observed (8, 9). Both these intensities decrease with an increase in shortening velocity of contracting muscle (101). They are close to their relaxed values during contraction at maximal velocity (87).

In early synchrotron experiments with 1D x-ray detectors no visible increase in I_{A1} during development of isometric contraction was found (5). A model was suggested to explain this finding. A significant fraction of myosin heads in contracting muscle was assumed to be non-stereo-specifically bound to actin (102). More recently with the advent of 2D x-ray detectors an increase in I_{A1} during isometric contraction was observed (103). Using highly collimated x-ray beam, two neighboring layer lines, M1 (at ~43 nm) and A1 (at ~36 nm) in contracting muscle were reliably resolved and their intensities in different states were measured (47). In frog muscle contracting at low temperature I_{A1} is 10-15% of that in rigor (54, 8). When the temperature of contracting muscle increases, I_{A1} also increases in parallel with tension while the number of myosin heads bound to actin, as estimated from stiffness measurements, remains constant (7, 8, 65, 66). At high temperature I_{A1} in isometrically contracting fibers from frog and rabbit muscles is about one third of its rigor value (8, 9). During shortening of contracting muscle under very low load I_{A1} decreases by a factor of ~2 (47) in parallel with the decrease in the number of myosin heads bound to actin (104). Other actin layer lines: A2, A4, A5 are also present in the diffraction pattern of contracting muscle (47, 54). Their intensities increase in parallel with tension when the temperature of contracting muscle increases (9).

Some actin layer lines are insensitive to the conformation of myosin heads strongly bound to actin while others provide information about these conformational changes. The intensity profile of the 1st actin layer line A1 was shown to be independent of a 30-35° tilt of the lever arm of myosin heads strongly bound to actin (20). The theory readily explains this by the fact that its pitch, ~36 nm, is much longer than the lever arm, ~10 nm (63, 61). More pronounced changes caused by the tilt were observed on the A2, and especially on the higher order actin layer lines, A5-A7, as they have spacings close to the size of the lever arm and for this reason are sensitive to its axial and azimuthal tilt (20).

The intensities of the actin layer lines, especially of A1, can be used to estimate the number of myosin heads bound to actin. The so called 'square law' assumes that the intensity of a layer line is proportional to the square of the number of myosin heads strongly bound to actin (103, 7, 8, 47, 17). However it was shown that for some actin layer lines, including A1, the square law is not correct as the binding pattern of myosin heads to actin is not random, but has modulation with myosin-based periods of ~14/5 nm and ~7.25 nm (63, 78, 105). An attempt to measure the dependence of the intensities of the actin layer lines on the degree of actin occupancy by strongly bound myosin heads was made by Tamura *et al.* (19). For this, different amounts of S1 were added to myosin fibers stretched to non-overlap sarcomere length in the presence and in the absence of Ca^{2+}. It was found that the system saturates at an actin to S1 ratio of 0.3-0.4, that is far below full actin saturation and the intensities follow a linear rather than a square relationship. The authors explained their results by cooperative non-random S1 binding to actin and by blocking of S1 diffusion into myofibrils after a critical concentration of bound heads is achieved (*ibid.*).

The contribution of non-stereo-specifically bound heads to the actin layer line intensities in contracting muscle is sometimes controversial (88). The absence of the shift of the position of the intensity peak on A6 in contracting muscle can possibly be accounted for by non-stereo-specific binding (17). Some authors believe that the lattice sampling by the layer lines affects their intensities, although it was shown theoretically that, in contrast to the equatorial and meridional reflections, their total integral intensity does not depend on the lattice disorder and sampling (63).

3.3.3. Actin-myosin beating layer lines

The presence in the diffraction pattern from rigor muscles of the off-meridional layer lines with spacings of ~23-24 nm and ~10.2-10.4 nm that are not multiples of a period of either actin or myosin structures was discovered by Huxley and Brown (26). Bordas and colleagues (54) found that these layer lines which are absent in the relaxed pattern appear when muscle develops active tension (see also Figure 1). Later Yagi (106) explained the origin of these layer lines (he called them beating layer lines) by modulation of the actin binding pattern by myosin heads with a myosin-based periodicity on the basis of a theoretical approach (107). The most prominent myosin period, ~14.5 nm, i.e. the distance between neighbor crowns of myosin heads, is the main source of such modulation. The modulation results in the appearance of the layer lines with axial spacings of $\sim 1/14.5\ nm^{-1} - \sim 1/36\ nm^{-1} = \sim 1/24\ nm^{-1}$, AM_{-1}, and $\sim 1/14.5\ nm^{-1} + \sim 1/36\ nm^{-1} = \sim 1/10.4\ nm^{-1}$, AM_{+1}, where 36 nm is the pitch of the actin helix. The only possible origin for these layer lines is myosin heads that are bound to actin and adopt the actin-based helical order, modulated by the myosin-based ~14.5 nm period. Neither unbound heads nor thin filaments themselves contribute to these layer lines. The theory of the beating layer lines was further developed to account for non-periodic binding modulation (108). More recently, a comprehensive theory with explicit expression for the layer line intensities for partially occupied helices and taking into account both the 14.5 nm and 7.25 nm modulations which arise from the three-dimensional structure of the filament lattice in the A-band was described (105, 63, 78).

4. TIME-RESOLVED X-RAY DIFFRACTION OF CONTRACTING MUSCLE

The high brilliance of new synchrotron radiation sources opened exciting possibility to study the dynamics of molecular movement in contracting muscles or single muscle fibers using time-resolved x-ray diffraction. To monitor the time course of structural changes in a significant fraction of myosin heads these changes should be synchronized by step changes in mechanical, thermal or biochemical states which control the timing of actin-myosin interactions. In this case the time course of structural changes can be monitored concomitantly with those of tension and sarcomere length for understanding the relation between structure and mechanical function.

4.1. Mechanical transients

4.1.1. Transients induced by step releases or stretches

An approach to synchronization of crossbridge responses was first put forward by Huxley and Simmons (109) who applied sudden step changes in the length of a single skeletal muscle fiber of the frog during the plateau of a fused tetanus and measuring tension transients induced by length perturbations in the range of ±0.5% of the fiber length. The main features of the tension transients following fast length perturbations were described in detail and interpreted in terms of crossbridge behavior. The transients induced by step releases consisted of elastic response (phase 1) followed by a fast partial tension recovery with a rate constant of ~1000 s^{-1} (phase 2). For the next several milliseconds tension remains nearly constant (phase 3) before it recovers completely to its initial level with a rate constant of 10-100 s^{-1} (phase 4). The rate constant of phase 2 increases with the extent of fiber release and decreases after stretches. Based on these experiments a model for the force generating mechanism by the crossbridges was proposed (109). In the model, a solid crossbridge rotates about a point of attachment on the thin filament through a number of discrete states like a ratchet, and stretches an elastic element connecting it with the rod of the thick filament. Phase 2 is considered to result from force generating steps of attached crossbridges while the final tension recovery represents a change in the crossbridge population that accompanies their detachment and reattachment.

The structural evidence supporting this model was first obtained in time-resolved x-ray diffraction experiments with whole frog muscle (4, 5). It was found that the intensity of the M3 meridional reflection (I_{M3}) that corresponds to a ~14.5 nm axial repeat of myosin molecules along the backbone of the thick filament transiently decreases after step releases and stretches. However, for small amplitude releases (2-3 nm per half-sarcomere) no decrease in I_{M3} was detected and even some increase in I_{M3} has been observed (5, 57, 68, 112). For stretches or releases of larger amplitude I_{M3} does decrease (4, 5, 112). Experiments with single muscle fibers with submillisecond time resolution have demonstrated that the decrease in I_{M3} after the step releases occurs synchronously with phase 2 of the tension transient (67).

Changes in I_{M3} upon length perturbations were interpreted as evidence for an axial movement of the myosin heads associated with mechanical execution of working stroke (5, 67, 112, 68). The asymmetric behaviour between the stretches and releases gives an indication of the average orientation of attached myosin heads in contracting muscle (112, 68, 57, 69). It is believed that in average LCD is tilted slightly towards the M-line (57, 69, 2).

After step length changes, I_{M3} recovered partially in 5-10 ms after releases and in 30-50 ms after stretches. The recovery time coincides with the time of 'repriming' of the force responses to length step changes (110, 111). Final I_{M3} recovery has the same time course as phase 4. It was also found that a decrease in I_{M3} following a release or

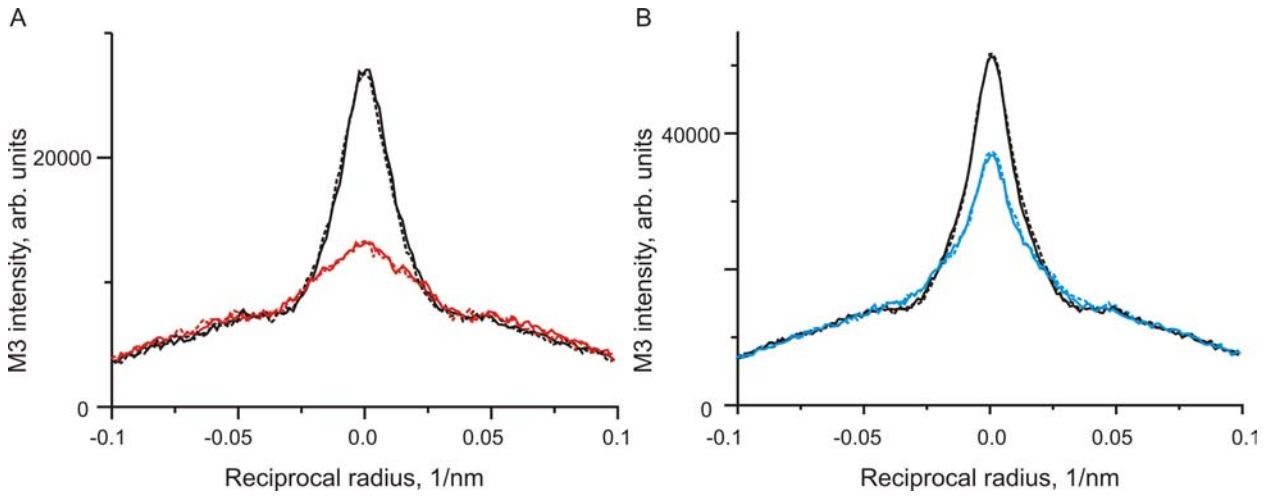

Figure 6. Radial profiles of the M3 meridional reflection during isometric contraction (black) and after releases (blue) or stretches (red) of bundles of three permeabilized fibers from rabbit muscle at ~30 °C. Data collected on ID02 at the ESRF from 4 bundles in each of two series of experiments with a CCD detector. Step stretches by 4.5-5.5 nm per half-sarcomere (A) or releases by 8.5-10.5 nm per half-sarcomere (B) were applied. Pre-step (black) profiles were collected in 4 ms long time frames; the post-step (color) profiles were collected in 2 ms long frames immediately after the end of the step. Continuous and dashed lines correspond to the M3 reflections in each half of the un-mirrored patterns.

stretch is reversible if muscle length is returned to its initial level in 1-2 ms after the length step (5). This change in I_{M3} becomes irreversible if the time interval between two length steps is long enough (5, 111).

Length step releases induce a decrease in I_{M3} only during phase 2 of the tension responses while no changes were seen during the step itself in phase 1 (67). Later a change in I_{M3} during phase 1 was found in responses to both releases and stretches only when the period between the subsequent length steps was short (111). Terms 'long' and 'short' relate to the 'repriming' time (110). The repriming is possibly accompanied by a detachment and attachment of myosin heads and a change in the population of attached heads (113). An explanation of the dependence of I_{M3} on the interval between length steps by incomplete reattachment of myosin heads in short stretch-release cycles is supported by the observation that the recovery of I_{M3} after length perturbations in frog muscle has a time course similar to that of the 'repriming' (5, 111).

No changes in the width of the M3 meridional reflection in the radial direction was found in response to length steps in early experiments (5, 112). Recently an increase in the M3 intensity in the region of the 1,0 row line was observed in contracting intact frog muscles after quick releases (61). Our experiments with bundles of three permeabilized fibers from rabbit muscle contracting at ~30 °C also show a widening of the M3 reflection after both releases and stretches (Figure 6). It is seen that after the step changes the M3 intensity profile becomes not Gaussian, with a more complex shape possibly arising from two different structures with different average radii. We cannot exclude unlikely possibility that the change in the M3 width and shape is a specific feature of multi-fiber specimens (ref. 61; Figure 6) and are absent in single fibers. However data from single fibers presented in (112) are too noisy to see the fine changes in the M3 shape described above (Figure 6; ref. 61).

Apart from the large changes in the intensity of the M3 meridional reflection, the brightest non-equatorial reflection in the diffraction pattern of contracting muscle, changes in other myosin reflections following a length step have been reported. The intensity of the M2 'forbidden' reflection increases upon step stretches (5, 61). No changes in the intensity of the M6 meridional reflection, I_{M6}, were found in early length step experiments (5). However in more recent experiments performed on the 3rd generation synchrotrons, up to a 60% increase in I_{M6} was observed upon releases (57, 61) and a ~20% decrease upon stretches (61).

Another recent finding concerns changes in the intensity, I_{AM+1}, of the beating AM_{+1} actin-myosin layer line at ~10.4 nm that decreases by ~80% upon releases and by 30-50% upon stretches (61, 117). The authors interpreted these changes in I_{AM+1} as a sign of lever arm tilt. Small changes in the intensity of the actin A6 layer line following length steps were also reported (*e.g.* 61).

4.1.2. Transients induced by sinusoidal length oscillations

In rigor where all myosin heads are bound to actin filaments and are believed to be in the final force-bearing state of the crossbridge cycle, I_{M3} changes in-phase with tension and sarcomere length in response to 3 kHz sinusoidal length oscillations of single muscle fibers. During contraction, I_{M3} changes in antiphase with 16 μs precision (2). The purpose of the experiments was to isolate the elastic behaviour of the myosin heads and to reduce the contribution of active force recovery. These observations

were analyzed assuming that in rigor the head conformation is the same as that suggested from fitting atomic structures to EM data (118) and that only the LCD participates in the tilting motion. It was estimated that in contracting muscle the axis of LCD, or 'lever arm', is at a slightly off-perpendicular angle with respect to the fiber axis, being tilted by ~8° from perpendicular towards the M-line. This suggests a ~30° in tilt LCD between rigor and its average conformation in contracting muscle (2).

A detailed study of the dependence of changes in I_{M3} on the frequency and amplitude of applied sinusoidal oscillations of fiber length has shown a more complicated and nonlinear behavior in the conditions where active tension recovery and a reattachment of myosin heads to 'new' actin sites is expected (69). In the frequency range from 100 Hz to at least 1 kHz, a significant deviation from sinusoidal I_{M3} response was observed: it decreased roughly sinusoidally during positive phase of length change but its increase during the negative phase was greatly distorted, forming a double peak. A decrease in amplitude or an increase in frequency lead to a reduction in the distortion while at ~3 kHz the changes became almost sinusoidal as had been reported earlier (2). The amplitude of I_{M3} changes was found to be frequency dependent with a ~3 fold decrease for an increase in frequency from 100 Hz to ~3 kHz (69). The experimental results were analyzed using a static model similar to that proposed by Dobbie *et al.* (2). The frequency dependence of the I_{M3} amplitude was explained by an increasing contribution of the power stroke or quick tension recovery at lower frequency, relative to the pure elastic distortion measured at high frequency (69).

Oscillations in I_{M3} in response to applied low-amplitude 1 kHz sinusoidal oscillations of the fiber length were found to be temperature dependent (70). At 4ºC the I_{M3} oscillations were in antiphase with the applied length changes and more or less sinusoidal. At 12ºC an extra drop in the positive wave of the I_{M3} signal appeared and at 22ºC the amplitude of this drop became equal to the amplitude of the main wave so that the frequency of the I_{M3} oscillations doubled. The results were interpreted as evidence for a tilt of the light-chain domain into a more perpendicular orientation at higher temperature (70).

4.1.3. Interference studies

The new interferometry technique was first used in experiments with step-length changes in intact frog single fibers (3). Quick releases were applied to isometrically contracting fibers and short x-ray frames were recorded during phase 1 and phase 2 of the tension transients. Changes of the interference distance L were calculated from the changes in the ratio of high-angle and low-angle intensity peaks of the M3 reflection (see Figure 5). The changes in L include changes in axial position of an 'average' crossbridge together with changes in length of the thin and thick filaments. The estimated displacement of a crossbridge was about 1/5 of that applied to a half-sarcomere during phase 1. Although the filament compliance was estimated to be 60% of the total half-sarcomere compliance a two-fold discrepancy between observed and expected changes in M3 interference splitting remained. To resolve the discrepancy the authors of (3) assumed that only one head of a myosin molecule binds actin during muscle contraction while its partner detached head remains nearly perpendicular to the filament axis with a narrow angular distribution. The second head contributes to I_{M3} substantively and according to the assumption does not move in response to applied length changes.

The change in the M3 interference profile during phase 2, i.e. quick partial tension recovery following a step shortening was nearly invisible (3). As phase 2 is believed to be the working stroke of crossbridges (109), the apparent absence of the axial movement of the 'average' crossbridge was unexpected. This observation was explained by the effect of filament compliance and contribution of detached partners of attached myosin heads to the M3 intensity (3).

Changes in the interference profiles of the M3 and M6 reflections in response to length changes of different size applied to contracting whole muscle were studied by H.E. Huxley and colleagues (119, 120, 57). Quick releases and steady shortening also induced only small changes in the interference fringes of the M3 and M6 intensities. A model similar to (3) was used by the authors for data interpretation and a significant contribution from some immobile structures to both reflections was assumed to explain the small apparent crossbridge displacements. The experiments with load step changes applied to isometrically contracting intact single muscle fibers were designed to eliminate the contribution of filament compliance (6). Changes in the interference splitting during phase 2 of length transient should reflect directly the extent of the working stroke as the filament strain remains constant and detachment/reattachment of the heads is negligible at this short time interval (5, 110). A 4 nm filament sliding during phase 2 under constant low load was accompanied by a change in the interference pattern that corresponds to only about 1 nm change in the M3 interference distance. Again, to explain the data, a substantial contribution of detached myosin heads to the M3 intensity was assumed.

Models derived to explain the results of interference measurements have consequences that can be verified experimentally. For example, crossbridges with both heads nearly perpendicular to the filament axis should be seen in EM images of contracting muscle. Also model predictions of expected changes in the intensities of the high order myosin meridional reflections, M9, M15, and to actin layer lines A1 and possibly A6 could in principle be tested.

4.2. Temperature jump transients

Isometric tension developed by fully activated muscle fibers increases with temperature (121). In intact frog fibers in the temperature range of 2 ºC to 17 ºC tension increases by 43% (122) to 70% (66). In intact single rat muscle fibers tension was found to increase ~4.5 fold upon an increase in temperature from 5 ºC to 35 °C (123). Temperature jump (T-jump) applied to a chemically permeabilized fiber contracting at ~5ºC induces a tension rise. In frog muscle fibers tension increases by ~80% at

~30ºC (8). Up to 5-fold tension rise upon T-jumps from ca. 5ºC tp 37ºC was observed in rabbit muscle fibers (124, 125, 65, 9).

The T-jump induced tension rise accelerates with the final temperature, however it remains several-fold slower than that of the transient induced by a length step, and is strain-independent (65). In addition, these two types of transients do not interact and probably have a different origin (*ibid.*). This rise in tension in both rabbit and frog muscles occurs without any significant change in stiffness of fully activated fibers. This means that the number of myosin heads attached to actin filaments remains nearly constant and thus the rise in tension cannot be accounted for by an increase in this number (124, 7, 8, 65, 66). The average force produced by an attached myosin head increases with temperature so that structural changes responsible for this are of particular interest.

The tension rise following a T-jump induces a simultaneous decrease in the intensity of the 1,0 equatorial reflection without any significant changes in that of the 1,1 (7-9). Such behaviour of the equatorial intensities can be explained by a transition of non-stereo-specifically attached heads to a stereo-specifically bound state (7, 8). During such transition the catalytic domains of myosin heads remain in the vicinity of the thin filaments while their neck domains move away from the backbones of the thick filaments causing more pronounced decrease in the 1,0 intensity (7, 8)..

Changes in I_{M3} are biphasic: after T-jumps from ~5 ºC to ~30 ºC in rabbit muscle fibers, I_{M3} dropped by ~20% immediately after the T-jump and rose by ~60% with respect to its pre-T-jump level with a time course similar to that of the tension rise (9). An increase in the M3 intensity at higher temperature was also observed in intact muscle fibers where the increase was accompanied by an increase in its radial width (56). As the fraction of the bound myosin heads is temperature independent as it is seen from the constancy of stiffness and in the 1,1 intensity (7, 8, 9, 56), the increase in I_{M3} with temperature can be explained by either more perpendicular orientation of the heads with respect to the fiber axis or smaller dispersion from the 14.5 nm repeat. The dip in I_{M3} immediately after the T-jump demonstrates that the early phase of the tension rise is accompanied by a change in the axial orientation of myosin heads or their light chain domains (9).

It was found that tension rise after the T-jump in both frog and rabbit muscle fibers is accompanied by an increase in I_{A1} (7-9). This increase in I_{A1} is approximately proportional to that of tension and occurs simultaneously with it within 1 ms accuracy (9). A small increase in the intensity of all other actin layer lines up to A7 and in the beating actin-myosin layer lines AM_{-1} and especially AM_{+1} upon the T-jump was also observed (9). The changes in the layer line intensities took place without changes in the number of myosin heads bound to actin as estimated from the measurement of stiffness and equatorial x-ray intensities. Therefore they result either from conformational changes in the myosin heads bound to actin or from changes in the mode of their attachment to actin, i.e. from a rearrangement of the actin-myosin interface. A tilt of LCD of myosin heads with respect to CD that remains strongly bound to actin is expected to cause no changes in I_{A1} (61). This suggests that almost three-fold increase in I_{A1} after T-jump from 5 °C to 30 °C in rabbit muscle fibers can be only explained by a transition from a non-stereo- to a stereo-specifically bound state (9). Changes in I_{A1} upon T-jumps in frog fibers are slightly less pronounced (8). This correlates with smaller tension rise in frog muscle compared to rabbit one.

In rigor T-jump induced a drop in tension due to thermal expansion of the thin or/and thick filaments (124, 125). The only change in the rigor x-ray diffraction pattern observed upon T-jump is a decrease in the M3 intensity. This probably results from a release of strain in rigor myosin heads upon increase in temperature due to thermal expansion of myofilaments (8).

4.3. Flash photolysis of caged-compounds

A method of fast uniform activation of permeabilized (or demembranated) muscle fibers that synchronizes structural responses of myosin heads is to use a biologically inert molecule which upon illumination by a flash of light, breaks down to release an activator of muscle contraction. If this molecule diffuses freely into the muscle fiber, and if light pulse penetrates evenly throughout the fiber, fast and homogeneous activation ensues.

The most commonly used compound for this purpose is NPE-caged ATP, the $\underline{P}^3$-1-(2-nitrophenyl)ethyl ester of ATP (126), which photolyzes to ATP and the by-products 2-nitrosoacetophenone and H^+ (127). The appearance of ATP from NPE-caged ATP is temperature and pH dependent; it occurs with a rate constant of ~140 s^{-1} at pH 7.1 and room temperature (128). Depending on the absence or presence of calcium in the fiber, prior to photolysis, release of ATP results in relaxation (129, 130) or contraction (131), respectively. DMB-caged ATP that is P^3-[1-(3,5-dimethoxyphenyl)-2-phenyl-2-oxo]ethyl ester of ATP, liberates ATP faster than NPE-caged ATP with the dark reaction time >10^5 s^{-1} (132).

Early x-ray experiments with flash photolysis of caged-ATP were focused on relaxation kinetics of the equatorial intensities (10, 133-135). Later with the use of more advanced radiation sources and 2D x-ray detectors the intensities of the M3 meridional reflection and some layer lines were also resolved in the absence and in the presence of Ca^{2+} (11, 136, 137, 12-15). It was found that the decay of the rigor structure of actin filaments decorated by strongly bound myosin heads has a time course similar to that found in solution if the rate of ATP liberation and binding of caged-ATP to myosin are taken into account (15). No significant difference in the rate of ATP-induced acto-myosin dissociation between one-headed S1s and two-headed myosin molecules in muscle was found (*ibid.*). Fast DMB-caged ATP provides faster structural responses of muscle fibers than conventional NPE-caged ATP (12).

Experiments using arrays of single muscle fibers and a very bright light source showed that the intensity of the beating actin-myosin layer line AM_{+1} at ~10.4 nm decays slower than those of all actin layer lines upon ATP liberation in the absence of Ca^{2+} (15). As this layer line specifically indicates stereo-specific actin myosin bonds, the data show that rigor myosin heads switch on the thin filaments and activate normal contraction as was suggested by Goldman *et al.* (130).

Flash photolysis of caged-ATP in the presence of Ca^{2+} did not reveal a delay between ATP-induced dissociation of myosin heads from actin and their reattachment as estimated by the intensity of the 1st actin layer line A1 (12, 14). This probably results from insufficient spatial and temporal resolution of those experiments that makes it difficult to distinguish between the M1 and A1 layer lines.

Tension rise following photo-liberation of ATP in the presence of Ca^{2+} is accompanied by a rise in I_{M3} (136, 137, 14). A short dip in I_{M3} followed by its rise was resolved using fast DMB-caged ATP. It was also found that the rise in I_{M3} has the same rate constant as tension rise (12). These observations indicate that force generation is accompanied by a rearrangement of the cross-bridge orientation. The amount and the rate of the rise of I_{M3} correlate with those of tension in the experiments where tension rise was accelerated, but depressed by addition of 20 mM P_i in the pre-flash solution (14). The increase in I_{M3} during activation by flash photolysis of caged-ATP correlates with the amount of ATP liberated and becomes zero or even negative when [ATP] decreased to 0.13 mM or below (13). Changes in I_{A1} and I_{A6} upon liberation of small amounts of ATP were more pronounced than those of I_{M3} and equatorial intensities (*ibid*.).

Flash photolysis can also be used to change the concentration of other important components in the actomyosin ATPase cycle, such as ADP and inorganic phosphate. For instance Horiuti *et al.* (138) use caged-ADP to rapidly modify the ATPase product concentration in contracting muscle and to study its effect on the x-ray diffraction pattern. The photoliberation of ADP induced a fast drop of rigor tension and an increase in I_{M3} (138). The latter was similar to that achieved by a stretch of rigor muscle (139).

Muscle fibers can also be activated by photolytic release of calcium from caged-calcium. DM-Nitrophen is one such compound which releases calcium upon photolysis and induces muscle activation (140). It was used to show that the structural changes revealed by equatorial x-ray intensities precede force generation (141). Another caged-Ca compound, NP-EGTA, was used by Hoskins *et al.* (16) to investigate changes in the equatorial intensity profile induced by photolytically released calcium.

5. X-RAY DIFFRACTION AND MECHANISM OF THE ACTIN-MYOSIN MOTOR

5.1. X-ray diffraction on different muscle specimens

X-ray diffraction experiments performed with different muscle specimens gave similar, but not identical results. It is important to discuss possible effects of methodological differences on the observed diffraction patterns as it is believed that the structural changes which underlie observed changes in the pattern and the mechanism of the actin-myosin motor in different muscles is universal.

Intact frog muscle is the classic object of x-ray diffraction studies (1, 24-26,). More recently when modern high flux synchrotron radiation sources with a small beam size became available, single frog intact muscle fibers have been used by several research groups (2, 6, 22, 23, 42, 67, 69, 70). The main advantage of using single fibers instead of whole muscles is that changes in sarcomere length can be measured precisely using laser diffraction (42) or by means of a striation follower (67). Oxygenation of a single fiber is easier than that of a whole muscle so that one can expect higher ATP concentration and lower concentrations of the products of its hydrolysis during contraction of a single muscle fiber. Electrical stimulation of a single fiber is also more reliable. In whole muscle preparations a failure to respond to stimulation of a small fraction of the fibers is difficult to detect although even a small fraction of fibers that fail to be activated corrupt the x-ray diffraction pattern of contracting whole muscle. The use of small bundles of intact fibers (33) is a reasonable compromise especially if the size of synchrotron x-ray beam is too large and its flux is not high enough for a single fiber.

It is worth mentioning that many x-ray diffraction experiments with intact frog muscles and single fibers were performed at a low temperature at which frogs are able to crawl, but not jump. Only in a few papers more physiological temperature has been explored (56, 70, 92,).

The diffraction pattern of contracting intact mammalian muscle from mice diaphragm was described by Iwamoto *et al.* (159). The pattern collected from this muscle during isometric contraction at 25 °C was similar to those obtained from intact frog muscles contracting at 5 °C. The only difference found is a significant contribution of the M6 layer line to the off-meridonal intensity of the combined A5/M6 layer line in the frog sartorius, but not in mouse diaphragm muscle (159).

Whole muscles, single fibers or small bundles of fibers from mammalian muscles with permeabilized cell membrane are also classical preparations for x-ray diffraction studies on muscle (67). An advantage of using muscle specimens with permeabilized membrane is that the chemical environment of contractile proteins can be controlled. The loss of electrical excitability of the fibers is also convenient for using flash photolysis of caged compounds and joule temperature jump techniques described above in sections 4.2, 4.3. A majority of biochemical studies of the actin-myosin ATPase in solution and in muscle fibers were performed with rabbit skeletal myosin or fibers from rabbit muscle, so that the kinetic properties of these specimens are well documented and can be compared with the time course of structural changes revealed by x-ray diffraction.

A disadvantage of permeabilized muscle preparations is that diffusion of ATP and products of its hydrolysis may be insufficiently fast for maintaining the chemical potential of the actin-myosin ATPase. For maintaining a high concentration of ATP and a low concentration of ADP, high concentration of phosphocreatine-phosphokinase backup system is needed (29, 160), although the presence of some inorganic phosphate in the core of a single fiber is unavoidable (161). The diffusion problem becomes worse when bundles of muscle fibers are used instead of a single fiber because the diffusion rate is proportional to the square of the muscle diameter. Besides cell membranes in multi-cellular specimens hamper diffusion even after the membranes are made permeable. A compromise between the diffusion problem and low diffracting power of single fibers can be achieved by using an array of single muscle fibers (17, 18, 20) although dissection and mounting of such array is difficult and time consuming. The use of small bundles of two-four fibers (9, 158) is another reasonable compromise between diffusion rate and diffracting power. However special efforts are needed to assure homogeneity of sarcomere length of different fibers in the bundle (9).

The main problem in using fibers with permeabilized membranes is the loss of their structural homogeneity during activation by Ca^{2+}. This problem is especially serious in frog fibers where wide dispersion of sarcomere length takes place even at partial Ca-activation (162). The sarcomere disorder is also quite severe for mammalian muscle fibers if they are activated at temperature above 10-15 °C (163). To overcome this problem, sarcomere structure can be stabilized, and incipient disorder during force development minimized by treating fibers with EDC (29, 164) using a modification of the procedure initially suggested by Tawada and Kimura (165). EDC covalently cross-links amino groups on side chains of a protein to carboxylic side chain of another protein. It was shown to cross-link lysines of loop 2 on a myosin heads to acid residues on the N-terminus of actin (166). EDC also induces some cross-linking within the thin filaments and partially switching them on even in the absence of Ca^{2+} (165).

Although EDC treatment protects structural homogeneity of muscle fibres during Ca^{2+} activation, there is concern relating to the extent of modification of the mechanical and structural properties of the fibers by EDC cross-linking. The extent of cross-linking was estimated by measuring instantaneous stiffness of muscle fibres in the 'super-relaxing' solution, i.e. in the absence of Ca^{2+} and in the presence of high concentrations of inorganic phosphate, P_i, and butanedione-monoxime, BDM (29). BDM and P_i were added to prevent binding of uncross-linked myosin heads to thin filaments partially switched on by the EDC treatment. After treatment of frog fibers with 10 mM EDC for 10 min some active tension and stiffness have been detected in the 'super-relaxing' solution. Tension was below 10% and instantaneous stiffness was between 12% and 20% of the value during isometric contraction at saturating concentration of Ca^{2+} (29). In another set of experiments with frog muscle fibers with longer EDC treatment (10-15 min) ~5% remaining tension and 13-19% remaining stiffness were found in the 'super-relaxing' solution compared to fully Ca-activated contraction. As about a half of half-sarcomere compliance in contracting muscle is due to filament compliance (8) these stiffness measurements suggest that about 10% of myosin heads were cross-linked to actin in these conditions.

The effect of EDC cross-linking on the diffraction pattern is discussed below. The fact that most myosin heads remain uncross-linked (>10:1) and cycle in a normal way is supported by the results of length step experiments (29). Changes in I_{M3} following length releases and stretches of EDC treated fibers from frog (29, 8) and rabbit (ref. 9; Figure 6) muscles are very close to those in intact frog muscles (57) and single fibers (112). It should be noted that for rabbit muscle fibers, a shorter EDC treatment than for frog fibers is needed (5-6 min compared to 10-15 min) to protect structural order (9) because of much lower relative force they develop at decreased temperature of activation.

An increase in I_{A6} intensity and the amount of the A1 component in the combined A1/M1 layer line in the 'super-relaxing' solution after EDC treatment for 6.5 min compared to relaxed pattern before the treatment shown in Figure 7. Increase in I_{A6} was only 7% (Figure 7*C*). This figure is much lower than the increase in I_{A6} during the transition of the same muscle bundle to rigor (87%, Figure 7*C*) and significantly less than *ca*. 40% increase in I_{A6} upon development of isometric contraction. A 6-7% increase in I_{A6} was found upon activation of the thin filaments without attachment of myosin heads (93, 17, 158). As EDC treatment was shown to cross-link regulatory proteins (167) the data presented in Figure 7C demonstrates that only a small minority of myosin heads were cross-linked to actin.

The heads cross-linked to actin with EDC in rigor are also expected to increase the A1 component in the combined first actin-myosin layer line. In the 'super-relaxing' solution the A1 component however was not seen (Figure 7*B*). A small shoulder corresponding to 2.3% of the rigor A1 intensity can be detected by fitting the M1/A1 layer line with fractions of the A1 (rigor) and M1 (relaxed) component (Figure 7*B)*. This is much smaller than the 30% contribution of the rigor A1 intensity in the same combined actin-myosin layer line during isometric contraction at near-physiological temperature (Figure 7*A*). The data confirm that limited treatment with EDC only marginally affects the x-ray diffraction pattern of muscle fibers. It was shown (7, 8, 29) that the ability of muscle fibers to respond to small perturbations (<10 nm per half-sarcomere length) also remains unchanged although the fibers cannot shorten by more than 1.5% of their length.

5.2. Structural models of the actin-myosin motor in muscle

Different orientations of crossbridges in rigor and relaxed states first found in flight insect muscle (142) gave rise to the swinging crossbridge hypothesis (143). In this hypothesis, the head of a myosin molecule turns as a whole around its point of attachment to the thin filaments thus

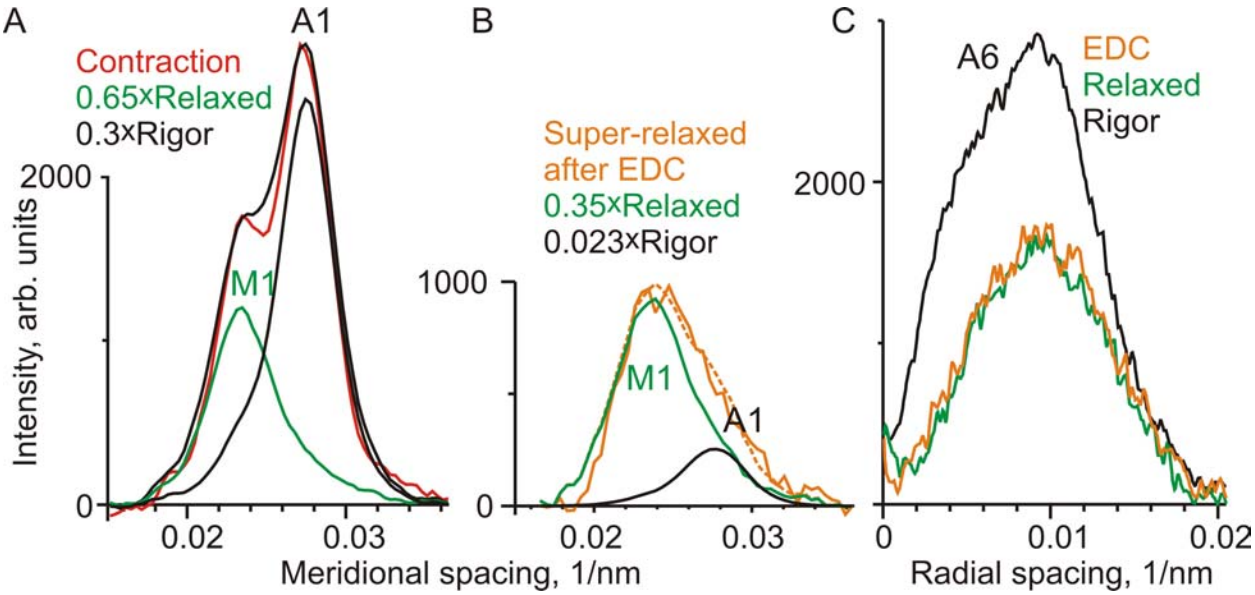

Figure 7. Effect of EDC cross-linking on the intensities of some actin layer lines. A: The region of the first myosin (M1) and actin (A1) layer lines on the 1,1 row line. Off-meridional integration in the region of reciprocal radii from 0.035 nm^{-1} to 0.06 nm^{-1}. The same data set as in Figure 1. Intensity profile during contraction at 30 °C after 5.5 min treatment with EDC (red) was fitted by a wighted sum of the relaxed (green) and rigor (black) intensities measured before EDC cross-linking. The relaxed and rigor intensity approximately correspond to the M1 and A1 components. B and C: data from a bundle of three fibers in relaxing (green), rigor (black) and 'super-relaxing' (brown) solutions. Data in super-relaxing solutions wee obtained for 200 ms after treatment with 10 mM of EDC for 6.5 min. In *B* the same integration region and the same deconvolution procedure as in A was employed. In *C* the A6 layer line was integrated along the meridian and plotted against reciprocal radius. Background is subtracted.

pulling the two filaments along each other. This concept was later used for explaining tension transients induced by step length changes of contracting muscle (109).

The crystal structure of myosin subfragment 1, S1, revealed that the molecule consists of two main fragments – a globular catalytic, or motor, domain which binds actin and hydrolyzes ATP and a light chain domain, LCD, that is long α-helical heavy chain neck with essential and regulatory light chains bound (118). The angle between the two domains was found to change depending on nucleotide bound to the active site of S1 (144-146). These findings lead to so called 'lever arm' hypothesis. According to it force generation by myosin S1 results solely from a tilt of the light chain domain with respect to the motor domain bound to actin filament (147, 114-116). Changes which occur in the actin-myosin interface were by default supposed to be not important for mechanical function of the motor. As the hypothesis arose from crystallographic data obtained with S1 in the absence of actin, its independent verification in muscle, i.e. in the conditions where myosin motors produce mechanical work, is of particular importance.

A number of experimental results are in line with the 'lever arm' hypothesis. Among them is a tilt of rhodamine probes attached to the light-chain domain as measured by fluorescence polarization (148-150) and changes in the M3 intensity on x-ray pattern upon step length changes (5, 67). Also the unloaded velocity of actin filaments on myosin-coated surface in the *in vitro* motility assay was found to be directly proportional to the length of engineered LCD (151). All these data support but do not prove the lever arm hypothesis as can be interpreted by swing of whole S1 on the actin surface.

There are however several observations that do not fit the lever arm model. EM tomograms of quickly frozen contracting insect flight muscles show a wide distribution of the azimuthal and axial angles of attachment of myosin motor domains with respect to actin (152), suggesting a rolling of the catalytic domain of myosin head on the actin surface (153). In optical trap experiments the working stroke of S1 from myosin II molecule with truncated LCD was found to be larger than the size of the interdomain bending predicted by the lever arm mechanism (154).

Direct x-ray evidence for two different ways of binding myosin heads to actin was obtained in T-jump experiments on single muscle fibers from the frog (7, 8). It was found that the tension rise after the T-jump is accompanied by an increase in the intensity of the first actin layer line, I_{A1}. Such an increase in the diffracting power of the actin helix for a constant number of attached myosin heads (8, 65, 66) can be explained by a change in the mode of binding of myosin heads. The long pitch of the actin helix, ~36 nm, is much longer than LCD (~10 nm).

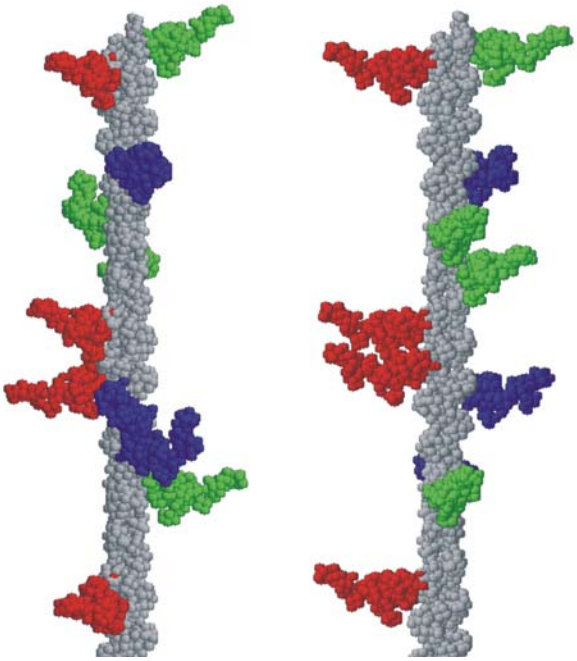

Figure 8. On the right, myosin heads are stereo-specifically bound to actin. The actin-S1 interface is as suggested by Holmes *et al.* (156), with the lever arms of the heads tilted axially by 50° compared to their rigor state. On the left, the myosin heads are bound non-stereo-specifically to the same sites on an actin filament. Blue, red and green myosin heads are coming from the three surrounding myosin filaments. The actin filament is shown in grey. The non-stereo-specifically bound heads are attached to actin over a range of azimuthal and axial angles. M-line is on the top.

For this reason, any possible lever arm tilt in the axial or azimuthal directions does not affect the A1 intensity (63, 61, 78). These data suggest that the heads which were initially attached to actin non-stereo-specifically, i.e. at different azimuthal and maybe axial angles, gain the order defined by the actin helix, i.e. bind actin stereo-specifically (Figure 8).

When axial and especially azimuthal angles between S1 motor domain and actin deviated from their fixed values characteristic for stereo-specific binding, the intensities of the actin layer lines decrease because of the loss of actin helical symmetry. A transition of non-stereo-specifically bound myosin heads to a stereo-specifically bound state leads to an increase in the intensities of the actin layer lines.

It was found that the time course of the increase in I_{A1} coincides with that of the tension rise with millisecond precision. in experiments where changes in force and in the x-ray diffraction pattern were monitored during isometric contraction of rabbit fibers with chemically permeabilized membrane in response to T-jumps from ~5 °C to ~30 °C (9). Although the time course of other actin and actin-myosin layer lines was not measurable in these experiments their intensity obviously also increased with tension. This confirms a rise in stereo-specific labeling of the actin helix. These observations lead to a new, 'roll and lock', model of force generation (*ibid.*). This model unites the transition from non-stereo-specific attachment to stereo-specific binding with the lever arm mechanism. It suggests that the stereo-specific 'locking' transition is accompanied by an axial swing of S1 and is an essential part of the force generation mechanism. The lever arm tilt occurs after this step. The model combines a Brownian ratchet mechanism used in the first model of actin-myosin motor (155) with the Huxley-Simmons type of model (109). In contrast to the original model (155) where the thermal driven movement of a cross-bridge was directed toward the M-line, in the 'roll and lock' model the Brownian movement is a rotation of a myosin head on actin surface. During the rotation the center of mass of the head moves toward the Z-line (9) with respect to the actin-S1 contact point. Correspondingly the center of mass moves M-ward with respect to the S1-S2 junction as suggested (70, 122). The model explains the observed changes in the intensities of a number of actin and myosin based x-ray reflections and predicts that the 'locking' transition should be strain-dependent (9). Changes in I_{A1} were found to accompany tension transients induced by length step perturbations of frog muscles (61, 117, 9) as predicted by the model. Releases increased I_{A1} while stretches decreased it by corresponding promoting and hampering the stereo-specific 'locking'.

It should be noted that experiments with fluorescent probes attached to SH1 group on CD of myosin heads in rabbit muscle fibers did not reveal any axial rotation upon length changes expected from the 'roll and lock' model (157). On the other hand, changes in the orientation of this probe induced by flash photolysis of caged-ATP and caged ADP did not correlate with changes in tension produced by myosin heads (157). This suggests that the probe rather reports local changes around the SH1 group and may be insensitive to a rotation of CD as whole.

The 'roll and lock' model suggests that initial binding of a myosin heads with ATP or ADP and P_i bound to actin may occur at a range of different azimuthal and axial angles, i.e. non-stereo-specifically. On the other hand, a number of experiments show a significant stiffness of the pre-force-generating myosin heads that is similar and probably equal to that of rigor, stereo-specifically bound heads (97). A question arises what is the nature of a non-stereo-specific weak actin-myosin bond and why its stiffness is high. Significant fraction of weakly bound myosin heads can be obtained in rabbit muscle fibers in the absence of Ca^{2+} at low temperature and low ionic strength (97, 98). Low temperature and high pCa ensure the absence of active tension, while the low ionic strength promotes binding of the heads to actin. The dependence of stiffness on the ionic strength indicates that the weak binding is presumably electrostatic. Instantaneous stiffness of muscle fibers in these conditions can be as high as 50% of its rigor value (97). The initial binding is believed to involve lysin rich loop 2 of CD of S1 and acid residues on the N-terminal of actin and probably on two other negatively charged spots formed by actin residues 24, 25 and 99, 100. Experiments with mutant proteins suggest that affinity of the weak actin-

myosin bond depends on the number of charges, but not on the detailed sequence (168, 169). The data imply that the electrostatic binding is probably non-stereo-specific and does not include a 'key and lock' type of protein-protein interaction. Molecular dynamic calculation showed that S1 loop 2 with positively charged residues is pointed away from the CD (170). This occurs due to electrostatic forces which pull charges away from the core of protein with low dielectric constant to solvent with high dielectric constant. The extended loop with positively charged residues acts as a feeler that senses negatively charged regions on actin and directs Brownian motion of the head toward them providing long range interaction and initial electrostatic binding. This involves forming of salt bridges and of probably hydrogen bonds between myosin loop 2. When the binding occurs the charged residues neutralize and the loop tends to collapse due to hydrophobic and van der Waals interactions. The bond that is formed after the collapse is non-stereo-specific as the particular set of the charged residues involved into interaction and the angle of attachment may vary significantly. On the other hand stiffness of such bond may be higher than stiffness of another region of a head, for example, bending stiffness of LCD. In thin case the total stiffness of a weakly and strongly bound head can be similar.

Interpretation of the x-ray diffraction data on muscle is unavoidably based on mathematical modeling. The models are based on known high resolution structures of myosin head and actin. Using these structures as 'brick' a one-dimensional (2, 6, 57, 58, 59, 60, 67) or three-dimensional (48, 61, 63, 78, 90) model can be built. Using the structural model the intensities of the x-ray reflections of interest are calculated. The majority of the models deal with only one or very few x-ray reflection. One-dimensional models which take into account only axial distribution of electron density are used for simulation of M3, sometimes M6 (57) and very occasionally higher order meridional reflections (59, 60). Space models which consider a thin filament with a set of myosin heads bound to it can simulate several meridional and layer line x-ray reflections (90, 61). More complicated model which takes into account three-dimensional filament lattice in the A-band of sarcomeres can explain the myosin-based modulation of binding of myosin heads to actin and is able to describe the whole 2D diffraction pattern of muscle including crystal-like lattice sampling (63, 78). Each model is based on a number of assumptions and additional parameters which characterize changes in the shape of myosin heads and its mode of attachment to actin, pattern of binding of myosin heads to actin, dispersion of actin-bound heads from 14.5 nm myosin based repeat, extensibility of the thin and thick filaments *etc*. Three-dimensional models which describe not only meridional, but also layer line reflections have an advantage of 1D models as they can be verified more accurately using all available experimental information.

The majority of models deal with a single 'average' crossbridge. It is assumed that the 'average' crossbridge is representative of the whole population, while the crossbridges may be distributed over different conformational states, strain, and deviation from myosin-based repeat and differently react to applied perturbations. For a single meridional reflection, one-dimensional model that involves tilting of myosin head or of its lever arm is sufficient, although new interference data require additional assumptions (3, 6, 57, 120). Experimental measurements taken from a single reflection are limited by its spacing, intensity and sometimes the ratio of interference sub-peaks. A number of model parameters should not exceed the number of experimentally measured values.

A complete description of the complex 3D machinery of actin-myosin interaction can be achieved only using all information from the x-ray diffraction pattern that can be obtained using up to date radiation sources and modern detectors and 3D models of structural changes underlying mechanical function of the motor.

6. ACKNOWLEDGEMENTS

We are very grateful to the team of station ID02 of the European Synchrotron Radiation Facility, particularly Drs. T. Narayanan, P. Panine, M. Roessle and Mr. J. Gorini as well as to Dr. W.I. Helsby from the detector group of Daresbury Laboratory (SRS) for excellent assistance during experimental sessions. We also thank Prof. J. Squire for providing us with bony fish muscles. Work was supported by MRC, RFBR, ESRF, grant of the President of Russian Federation.

7. REFERENCES

1. Huxley H.E.: Low-angle X-ray diffraction studies on muscle. *Disscus Faraday Soc* 11, 148 (1951)

2. Dobbie I., M. Linari, G. Piazzesi, M. Reconditi, N. Koubassova, M.A. Ferenczi, V. Lombardi & M. Irving: Elastic bending and active tilting of myosin heads during muscle contraction. *Nature* 396, 383-387 (1998)

3. Piazzesi G., M. Reconditi, M. Linari, L. Lucii, Y.B. Sun, T. Narayanan, P. Boesecke, V. Lombardi & M. Irving: Mechanism of force generation by myosin heads in skeletal muscle. *Nature* 415, 659-662 (2002)

4. Huxley H.E., R.M. Simmons, A.R. Faruqi, M. Kress, J. Bordas & M.H. Koch: Millisecond time-resolved changes in x-ray reflections from contracting muscle during rapid mechanical transients, recorded using synchrotron radiation. *Proc Natl Acad Sci U S A* 78, 2297-2301 (1981)

5. Huxley H.E., R.M. Simmons, A.R. Faruqi, M. Kress, J. Bordas & M.H. Koch: Changes in the X-ray reflections from contracting muscle during rapid mechanical transients and their structural implications. *J Mol Biol* 169, 469-506 (1983)

6. Reconditi M., M. Linari, L. Lucii, A. Stewart, Y.B. Sun, P. Boesecke, T. Narayanan, R.F. Fischetti, T. Irving, G. Piazzesi, M. Irving & V. Lombardi: The myosin motor in muscle generates a smaller and slower working stroke at higher load. *Nature* 428, 578-581 (2004)

7. Bershitsky S.Y., A.K. Tsaturyan, O.N. Bershitskaya, G.I. Machanov, P. Brown, R. Burns & M.A. Ferenczi: Muscle force is generated by myosin heads stereospecifically attached to actin. *Nature* 388, 186-190 (1997)

8. Tsaturyan A.K, S.Y. Bershitsky, R. Burns & M.A. Ferenczi: Structural changes in the actin-myosin cross-bridges associated with force generation induced by temperature jump in permeabilized frog muscle fibers. *Biophys J* 77, 354-372 (1999)

9. Ferenczi M.A., S.Y. Bershitsky, N. Koubassova, V. Siththanandan, W.I. Helsby, P. Panine, M. Roessle, T. Narayanan & A.K. Tsaturyan: The "roll and lock" mechanism of force generation in muscle. *Structure* 13, 131-141 (2005)

10. Goody R.S, K. Guth, Y. Maeda, K.J.V. Poole & G. Rapp: Time-resolved X-ray diffraction measurements on Lethocerus fibrillar flight muscle following the photolytic release of ATP from 'caged-ATP'. *J Physiol* 364, 75 (1985)

11. Poole K.J., Y. Maeda, G. Rapp & R.S. Goody: Dynamic X-ray diffraction measurements following photolytic relaxation and activation of skinned rabbit psoas fibres. *Adv Biophys* 27, 63-75 (1991)

12. Tsaturyan A.K., S.Y. Bershitsky, R. Burns, Z.-H. He & M.A. Ferenczi: Structural responses to the photolytic release of ATP in frog muscle fibres, observed by time-resolved X-ray diffraction. *J Physiol* 520, 681-696 (1999)

13. Horiuti K., N. Yagi & S. Takemori: Single turnover of cross-bridge ATPase in rat muscle fibers studied by photolysis of caged ATP. *J Muscle Res Cell Motil* 22, 101-109 (2001)

14. Yagi N., K. Horiuti & S. Takemori: Effects of inorganic phosphate on cross-bridge behavior after photorelease of ATP in permeabilized cells of rat skeletal muscle. *Pflugers Arch* 445, 238-245 (2002)

15. Wakayama J., T. Tamura, N. Yagi & H. Iwamoto: Structural transients of contractile proteins upon sudden ATP liberation in skeletal muscle fibers. *Biophys J.* 87, 430-441 (2004)

16. Hoskins B.K., C.C. Ashley, G. Rapp & P.J. Griffiths: Time-resolved X-ray diffraction by skinned skeletal muscle fibers during activation and shortening. *Biophys J* 80, 398-414 (2001)

17. Kraft T., T. Mattei, A. Radocaj, B. Piep, C. Nocula, M. Furch & B. Brenner: Structural features of cross-bridges in isometrically contracting skeletal muscle. *Biophys J* 82, 2536-2547 (2002)

18. Iwamoto H., K. Oiwa, T. Suzuki & T. Fujisawa: X-ray diffraction evidence for the lack of stereospecific protein interactions in highly activated actomyosin complex. *J Mol Biol* 305, 863-874 (2001)

19. Tamura T., J. Wakayama, T. Fujisawa, N. Yagi & H. Iwamoto: Intensity of X-ray reflections from skeletal muscle thin filaments partially occupied with myosin heads: effect of cooperative binding. *J Muscle Res Cell Motil* 25, 329-335 (2004)

20. Iwamoto H., K. Oiwa, M. Kovacs, J.R. Sellers, T. Suzuki, J. Wakayama, T. Tamura, N. Yagi & T. Fujisawa: Diversity of structural behavior in vertebrate conventional myosins complexed with actin. *J Mol Biol* 369, 249-264 (2007)

21. Huxley H.E.: Recent X-ray diffraction studies of muscle contraction and their implications. *Philos Trans R Soc Lond B Biol Sci* 359, 1879-1882 (2004)

22. Reconditi M.: Recent improvements in small angle x-ray diffraction for the study of muscle physiology. *Rep Prog Phys* 69, 2709-2759 (2006)

23. Lombardi V., G. Piazzesi, M. Reconditi, M. Linari, L. Lucii, A. Stewart, Y.-B. Sun, P. Boesecke, T. Narayanan, T. Irving & M. Irving: X-ray diffraction studies of the contractile mechanism in single muscle fibers. *Philos Trans R Soc Lond B Biol Sci* 359, 1883-1893 (2004)

24. Huxley, H.E.: Investigations in biological structures by X-ray methods. The structure of muscle. *PhD Thesis, University of Cambridge, Cambridge, UK* (1952)

25. Huxley H.E.: X-ray analysis and the problem of muscle. *Proc R Soc Lond B Biol Sci* 141, 59-62 (1953)

26. Huxley H. E. & W. Brown: The low-angle x-ray diagram of vertebrate striated muscle and its behaviour during contraction and rigor. *J Mol Biol* 30, 383-434 (1967)

27. Squire J.: The structural basis of muscular contraction. *Plenum Press*, NY (1981)

28. Malinchik S. & L.C. Yu: Analysis of equatorial x-ray diffraction patterns from muscle fibers: factors that affect the intensities. *Biophys J* 68, 2023-2031 (1995)

29. Bershitsky S., A. Tsaturyan, O. Bershitskaya, G. Mashanov, P. Brown, M. Webb & M.A. Ferenczi: Mechanical and structural properties underlying contraction of skeletal muscle fibers after partial 1-ethyl-3-[3-dimethylamino)propyl]carbodiimide cross-linking. *Biophys J* 71, 1462-1474 (1996)

30. Huxley H.E.: Structural difference between resting and rigor muscle; evidence from intensity changes in the low angle equatorial x-ray diagram. *J Mol Biol* 37, 507-520 (1968)

31. Haselgrove J.C. & H.E. Huxley: X-ray evidence for radial cross-bridge movement and for the sliding filament model in actively contracting skeletal muscle. *J Mol Biol* 77, 549-68 (1973)

32. Matsubara I., N. Yagi & H. Hashizume: Use of an X-ray television for diffraction of the frog striated muscle. *Nature* 255, 728-729 (1975)

33. Hoskins B.K., C.C. Ashley, R. Pelc, G. Rapp & P.J. Griffiths: Time-resolved equatorial X-ray diffraction studies of skinned muscle fibres during stretch and release. *J Mol Biol* 290, 77-97 (1999)

34. Vainstein B. K.+ Diffraction of X-rays by chain molecules. *Izdatelstvo Akademii Nauk SSSR, Moscow.* (1963)

35. Bennett P.M., A. Tsaturyan & S. Bershitsky: Rapid cryofixation of rabbit muscle fibres after a temperature jump. *J Microsc* 206, 152-160 (2002)

36. Squire J. & J. Harford: Muscle crossbridge positions from equatorial diffraction data: an approach towards solving the phase problem. *Adv Exp Med Biol* 170, 221-236 (1984)

37. Yu L.C. & B. Brenner: Structures of actomyosin crossbridges in relaxed and rigor muscle fibers. *Biophys J.* 55, 441-453 (1989)

38. Harford J.J. & J.M. Squire: Evidence for structurally different attached states of myosin cross-bridges on actin during contraction of fish muscle. *Biophys J* 63, 387-396 (1992)

39. Wray J.: Structure of relaxed myosin filaments in relation to nucleotide state in vertebrate skeletal muscle. *J. Muscle Res. Cell Motil* 8, 62 (1987)

40. Rapp G., M. Schrumpf & J.S. Wray: Kinetics of the structural changes in the myosin filaments of relaxed psoas fibers after a millisecond temperature jump. *Biophys J* 59, 35 (1991)

41. Matsubara I., Y.E. Goldman & R.M. Simmons: Changes in the lateral filament spacing of skinned muscle fibers when cross-bridges attach. *J Mol Biol* 173, 15-33 (1984)

42. Cecchi G., P.J. Griffiths, M.A. Bagni, C.C. Ashley & Y. Maeda: Time-resolved changes in equatorial x-ray diffraction and stiffness during rise of tetanic tension in intact length-clamped single muscle fibers. *Biophys J* 59, 1273-1283 (1991)

43. Fuchs F. & D.A. Martyn: Length-dependent Ca(2+) activation in cardiac muscle: some remaining questions. *J Muscle Res Cell Motil* 26, 199-212 (2006)

44. Farman G.P., E.J. Allen, D. Gore, T.C. Irving & P.P. de Tombe: Interfilament spacing is preserved during sarcomere length isometric contractions in rat cardiac trabeculae. *Biophys J* 92, L73-75 (2007)

45. Huxley H.E., A. Stewart, H. Sosa & T. Irving: X-ray diffraction measurements of the extensibility of actin and myosin filaments in contracting muscle. *Biophys J* 67, 2411-2421 (1994)

46. Wakabayshi K., Y. Sugimoto, H. Tanaka, Y. Ueno, Y. Takezawa & Y. Amemiya: X-ray diffraction evidence for the extensibility of actin and myosin filaments during muscle contraction. *Biophys J* 67, 2422-2435 (1994)

47. Bordas J., A. Svensson, M. Rothery, J. Lowy, G.P. Diakun & P. Boesecke: Extensibility and symmetry of actin filaments in contracting muscles. *Biophys J* 77, 3197-3207 (1999)

48. Takezawa Y., Y. Sugimoto & K. Wakabayashi: Extensibility of the actin and myosin filaments in various states of skeletal muscle as studied by X-ray diffraction. *Adv Exp Med Biol* 453, 309-316 (1998)

49. Tsaturyan A.K., N. Koubassova, M.A. Ferenczi, T. Narayanan, M. Roessle & S.Y. Bershitsky: Strong binding of myosin heads stretches and twists the actin helix. *Biophys J* 88, 1902-1910 (2005)

50. Linari M, I. Dobbie, M. Reconditi, N. Koubassova, M. Irving, G. Piazzesi & V. Lombardi: The stiffness of skeletal muscle in isometric contraction and rigor: the fraction of myosin heads bound to actin. *Biophys J* 74, 2459-2473 (1998)

51. Yagi N., E.J. O'Brien & I. Matsubara: Changes of thick filament structure during contraction of flog striated muscle. *Biophys J* 33, 121-138 (1981)

52. Squire J.M., J.J. Harford, A.C. Edman & M. Sjostrom: Fine structure of the A-band in cryo-sections. III. crossbridge distribution and the axial structure of the human C-zone. *J Mol Biol* 155, 467-494 (1982)

53. Martin-Fernandez M.L., J. Bordas, G. Diakun, J. Harries, J. Lowy, G.R. Mant, A. Svensson & E. Towns-Andrews: Time-resolved X-ray diffraction studies of myosin head movements in live frog sartorius muscle during isometric and isotonic contractions. *J Muscle Res Cell Motil* 15, 319-348 (1994)

54. Bordas J., G.P. Diakun, F.G. Diaz, J.E. Harries, R.A. Lewis, J. Lowy, G.R. Mant, M.L. Martin-Fernandez & E. Towns-Andrews: Two-dimensional time-resolved X-ray diffraction studies of live isometrically contracting frog sartorius muscle. *J Muscle Res Cell Motil* 14, 311-324 (1993)

55. Piazzesi G., M. Reconditi, I. Dobbie, M. Linari, P. Boesecke, O. Diat, M. Irving & V. Lombardi: Changes in conformation of myosin heads during the development of isometric contraction and rapid shortening in single frog muscle fibres. *J Physiol* 514, 305-312 (1999)

56. Brunello E., P. Bianco, G. Piazzesi, M. Linari, M. Reconditi, P. Panine, T. Narayanan, W.I. Helsby, M. Irving & V. Lombardi: Structural changes in the myosin filament and cross-bridges during active force development in single

intact frog muscle fibres: stiffness and X-ray diffraction measurements. *J Physiol* 577, 971-984 (2006)

57. Huxley H., M. Reconditi, A. Stewart & T. Irving: X-ray interference studies of crossbridge action in muscle contraction: evidence from quick releases. *J Mol Biol* 363, 743-761 (2006)

58. Linari M., G. Piazzesi, I. Dobbie, N. Koubassova, M. Reconditi, T. Narayanan, O. Diat, M. Irving & V. Lombardi: Interference fine structure and sarcomere length dependence of the axial x-ray pattern from active single muscle fibers. *Proc Natl Acad Sci U S A* 97, 7226-7231 (2000)

59. Juanhuix J., J. Bordas, J. Campmany, A. Svensson, M.L. Bassford & T. Narayanan: Axial disposition of myosin heads in isometrically contracting muscles. *Biophys J* 80, 1429-1441 (2001)

60. Oshima K, Y. Takezawa, Y. Sugimoto, T. Kobayashi, T.C. Irving & K. Wakabayashi: Axial dispositions and conformations of myosin crossbridges along thick filaments in relaxed and contracting states of vertebrate striated muscles by X-ray fiber diffraction. *J Mol Biol* 367, 275-301 (2007)

61. Yagi N., H. Iwamoto, J. Wakayama & K. Inoue: Structural changes of actin-bound myosin heads after a quick length change in frog skeletal muscle. *Biophys J* 89, 1150-1164 (2005)

62. Huxley H.E., A.R. Faruqi, M. Kress, J. Bordas & M.H. Koch: Time-resolved X-ray diffraction studies of the myosin layer-line reflections during muscle contraction. *J Mol Biol* 158, 637-684 (1982)

63. Koubassova N.A. & A.K. Tsaturyan: Direct modeling of x-ray diffraction pattern from skeletal muscle in rigor. *Biophys J* 83, 1082-1097 (2002)

64. Linari M., E. Brunello, M. Reconditi, Y.-B. Sun, P. Panine, T. Narayanan, G. Piazzesi, V. Lombardi & M. Irving: The structural basis of the increase in isometric force production with temperature in frog skeletal muscle. *J Physiol* 567, 459-469 (2005)

65. Bershitsky S.Y. & A.K. Tsaturyan: The elementary force generation process probed by temperature and length perturbations in muscle fibres from the rabbit**.** *J Physiol* 540, 971-988 (2002)

66. Piazzesi G., M. Reconditi, N. Koubassova, V. Decostre, M. Linari, L. Lucii & V. Lombardi: Temperature dependence of the force-generating process in single fibres from frog skeletal muscle *J Physiol* 549, 93-106 (2003)

67. Irving M., V. Lombardi, G. Piazzesi & M.A. Ferenczi: Myosin head movements are synchronous with the elementary force-generating process in muscle. *Nature* 357, 156-158 (1992)

68. Irving M., G. Piazzesi, L. Lucii, Y.B. Sun, J.J. Harford, I.M. Dobbie, M.A. Ferenczi, M. Reconditi & V. Lombardi: Conformation of the myosin motor during force generation in skeletal muscle. *Nat Struct Biol* 7, 482-485 (2000)

69. Bagni M.A., B. Colombini, H. Amenitsch, S. Bernstorff, C.C. Ashley, G. Rapp & P.J. Griffiths: Frequency-dependent distortion of meridional intensity changes during sinusoidal length oscillations of activated skeletal muscle. *Biophys J* 80, 2809-2822 (2001)

70. Griffiths P.J., M.A. Bagni, B. Colombini, H. Amenitsch, S. Bernstorff, C.C. Ashley & G. Cecchi: Changes in myosin S1 orientation and force induced by a temperature increase. *Proc Natl Acad Sci U S A* 99, 5384-5389 (2002)

71. Rome E.: Structural studies by x-ray diffraction of striated muscle permeated with certain ions and proteins. *Cold Spring Harbor Symp Quant Biol* 37, 331-339 (1972)

72. Rome E., T. Hirabayashi & S.V. Perry: X-ray diffraction of muscle labelled with antibody to troponin-C. *Nat New Biol* 244, 154–155 (1973)

73. Rome E., G. Offer & F. A. Pepe: X-ray diffraction of muscle labelled with antibody to C-protein. *Nat New Biol* 244, 152–154 (1973)

74. Haselgrove J.C.: X-ray evidence for conformational changes in the myosin filaments of vertebrate striated muscle. *J Mol Biol* 92, 113–143 (1975)

75. Malinchik S.B. & V.V. Lednev: Interpretation of the X-ray diffraction pattern from relaxed skeletal muscle and modelling of the thick filament structure. *J Muscle Res Cell Motil* 13, 406-419 (1992)

76. Reconditi M., N. Koubassova, M. Linari, I. Dobbie, T. Narayanan, O. Diat, G. Piazzesi, V. Lombardi & M. Irving: The conformation of myosin head domains in rigor muscle determined by X-ray interference. *Biophys J* 85, 1098-1110 (2003)

77. Hudson L., J.J. Harford, R.C. Denny & J.M. Squire: Myosin head configuration in relaxed fish muscle: resting state myosin heads must swing axially by up to 150 A or turn upside down to reach rigor. *J Mol Biol* 273, 440-455 (1997)

78. Koubassova N.A., S.Y. Bershitsky, M.A. Ferenczi & A.K. Tsaturyan: Direct modeling of x-ray diffraction pattern from contracting skeletal muscle. *Biophys J* (in press) (2008)

79. Xu S., S. Malinchik, D. Gilroy, T. Kraft, B. Brenner & L.C. Yu: X-ray diffraction studies of cross-bridges weakly bound to actin in relaxed skinned fibers of rabbit psoas muscle. *Biophys J* 73, 2292-2303 (1997)

80. Malinchik S., S. Xu & L.C. Yu: Temperature-induced structural changes in the myosin thick filament of skinned rabbit psoas muscle. *Biophys J* 73, 2304-2312 (1997)

81. Xu S., J. Gu, T. Rhodes, B. Belknap, G. Rosenbaum, G. Offer, H. White & L.C. Yu: The M.ADP.P(i) state is required for helical order in the thick filaments of skeletal muscle. *Biophys J* 77, 2665-2676 (1999)

82. Xu S., G. Offer, J. Gu, H.D. White & L.C. Yu: Temperature and ligand dependence of conformation and helical order in myosin filaments. *Biochemistry* 42, 390-401 (2003)

83. Urbanke C. & J. Wray: A fluorescence temperature-jump study of conformational transitions in myosin subfragment 1. *Biochemistry* 358, 165-173 (2001)

84. Yagi N.: Effects of N-ethylmaleimide on the structure of skinned frog skeletal muscles. *J Muscle Res Cell Motil* 13, 457-463 (1992)

85. Lovell S.J., P.J. Knight & W.F. Harrington: Fraction of myosin heads bound to thin filaments in rigor fibrills from insect flight and vertebral muscle. *Nature* 293, 664-666 (1981)

86. Ford L.E., A.F. Huxley & R.M. Simmons: Tension transients during steady shortening of frog muscle fibres. *J Physiol* 361, 131-150 (1985)

87. Yagi N., S. Takemori & M. Watanabe: An X-ray diffraction study of frog skeletal muscle during shortening near the maximum velocity. *J Mol Biol* 231, 668-677 (1993)

88. Xu S., J. Gu, G. Melvin & L.C. Yu: Structural characterization of weakly attached cross-bridges in the A*M*ATP state in permeabilized rabbit psoas muscle. *Biophys J* 82, 2111-2122 (2002)

89. Xu S., J. Gu, B. Belknap, H. White & L.C. Yu: Structural characterization of the binding of Myosin*ADP*Pi to actin in permeabilized rabbit psoas muscle. *Biophys J* 91, 3370-3382 (2006)

90. Gu J., S. Xu & L.C. Yu: A model of cross-bridge attachment to actin in the A*M*ATP state based on x-ray diffraction from permeabilized rabbit psoas muscle. *Biophys J* 82, 2123-2133 (2002)

91. Oda T., K. Namba & Y. Maeda: Position and orientation of phalloidin in F-actin determined by X-ray fiber diffraction analysis. *Biophys J* 88, 2727-2736 (2005)

92. Kress M., H.E. Huxley, A.R. Faruqi & J. Hendrix: Structural changes during activation of frog muscle studied by time-resolved X-ray diffraction. *J Mol Biol* 188, 325-342 (1986)

93. Yagi N. & I. Matsubara: Structural changes in the thin filament during activation studied by X-ray diffraction of highly stretched skeletal muscle. *J Mol Biol* 208, 359-363 (1989)

94. Wakabayashi K., H. Tanaka, Y. Amemiya, A. Fujishima, T. Kobayashi, T. Hamanaka, H. Sugi & T. Mitsui: Time-resolved x-ray diffraction studies on the intensity changes of the 5.9 and 5.1 nm actin layer lines from frog skeletal muscle during an isometric tetanus using synchrotron radiation. *Biophys J* 47, 847-850 (1985)

95. Kraft T., S. Xu, B. Brenner & L.C. Yu: The effect of thin filament activation on the attachment of weak binding cross-bridges: A two-dimensional x-ray diffraction study on single muscle fibers. *Biophys J* 76, 1494-1513 (1999)

96. Lymn R.W. & E.W. Taylor: Mechanism of adenosine triphosphate hydrolysis by actomyosin. *Biochemistry* 10, 4617-4624 (1971)

97. Brenner B., M. Schoenberg, J.M. Chalovich, L.E. Greene & E. Eisenberg: Evidence for cross-bridge attachment in relaxed muscle at low ionic strength. *Proc Natl Acad Sci U S A* 79, 7288-7291 (1982)

98. Brenner B., L.C. Yu & R.J. Podolsky: X-ray diffraction evidence for cross-bridge formation in relaxed muscle fibers at various ionic strengths. *Biophys J* 46, 299-306 (1984)

99. Brenner B. & L.C. Yu: Structural changes in the actomyosin cross-bridges associated with force generation. *Proc Natl Acad Sci U S A* 90, 5252-5256 (1993)

100. Matsubara I., N. Yagi, H. Miura, M. Ozeki & T. Izumi: Intensification of the 5.9-nm actin layer line in contracting muscle. *Nature* 312, 471-473 (1984)

101. Yagi N. & S. Takemori: Structural changes in myosin cross-bridges during shortening of frog skeletal muscle. *J Muscle Res Cell Motil* 16, 57-63 (1995)

102. Huxley H.E. & M. Kress: Crossbridge behaviour during muscle contraction. *J Muscle Res Cell Motil* 6, 153-161 (1985)

103. Yagi N.: Intensification of the first actin layer-line during contraction of frog skeletal muscle. *Adv Biophys* 27, 35-43 (1991)

104. Stehle R. & B. Brenner: Cross-bridge attachment during high-speed active shortening of skinned fibers of the rabbit psoas muscle: implications for cross-bridge action during maximum velocity of filament sliding. *Biophys J* 78, 1458-1473 (2000)

105. Tsaturyan A.K.: Diffraction by partially occupied helices. *Acta Crystallogr A*. 58, 292-294 (2002)

106. Yagi N.: Labelling of thin filaments by myosin heads in contracting and rigor vertebrate skeletal muscles. *Acta Crystallogr D Biol Crystallogr*. 52, 1169-1173 (1996)

107. Holmes K. C., R. T. Tregear & J. Barrington Leigh: Interpretation of the low angle x-ray diffraction from insect flight muscle in rigor. *Proc R Soc Lond B* 207, 13-33 (1980)

108. Gu J. & L.C. Yu: X-ray diffraction of helices with arbitrary periodic ligand binding. *Acta Crystallogr D Biol Crystallogr* 55, 2022-2027 (1999)

109. Huxley A.F. & R.M. Simmons: Proposed mechanism of force generation in striated muscle. *Nature* 233, 533-538 (1971)

110. Lombardi V., G. Piazzesi & M. Linari: Rapid regeneration of the actin-myosin power stroke in contracting muscle. *Nature* 355, 638-641 (1992)

111. Lombardi V., G. Piazzesi, M.A. Ferenczi, H. Thirlwell, I. Dobbie & M. Irving: Elastic distortion of myosin heads and repriming of the working stroke in muscle. *Nature* 374, 553-555 (1995)

112. Piazzesi G., V. Lombardi, M.A. Ferenczi, H. Thirlwell, I. Dobbie & M. Irving: Changes in the x-ray diffraction pattern from single, intact muscle fibers produced by rapid shortening and stretch. *Biophys J* 68, 92S-96S (1995)

113. Piazzesi G. & V. Lombardi: A cross-bridge model that is able to explain mechanical and energetic properties of shortening muscle. *Biophys J* 68, 1966-1979 (1995)

114. Holmes K.C.: The swinging lever-arm hypothesis of muscle contraction. *Curr Biol* 7, R112-R118 (1997)

115. Geeves M.A. & K.C. Holmes: Structural mechanism of muscle contraction. *Annu Rev Biochem* 68, 687–728 (1999)

116. Houdusse A. & H.L. Sweeney: Myosin motors: missing structures and hidden springs. *Curr Opin Struct Biol* 11, 182-194 (2001)

117. Yagi N., H. Iwamoto & K. Inoue: Structural changes of cross-bridges on transition from isometric to shortening state in frog skeletal muscle. *Biophys J* 91, 4110-4120 (2006)

118. Rayment I., W.R. Rypniewski, K. Schmidt-Base, R. Smith, D.R. Tomchick, M.M. Benning, D.A. Winkelmann, G. Wesenberg & H.M. Holden: Threedimensional structure of myosin subfragment-1: a molecular motor. *Science* 261, 50–58 (1993)

119. Huxley H.E., M. Reconditi, A. Stewart & T. Irving: X-ray interference evidence concerning the range of crossbridge movement, and backbone contributions to the meridional pattern. *Adv Exp Med Biol* 538, 233-241 (2003)

120. Huxley H., M. Reconditi, A. Stewart & T. Irving: X-ray interference studies of crossbridge action in muscle contraction: evidence from muscles during steady shortening. *J Mol Biol.* 363, 762-772 (2006)

121. Woledge R.C., N.A. Curtin & E. Homsher: Energetic aspects of muscle contraction. *Monogr Physiol Soc* 41, 1-357 (1985)

122. Linari M., E. Brunello, M. Reconditi, Y.B. Sun, P. Panine, T. Narayanan, G. Piazzesi, V. Lombardi & M. Irving: The structural basis of the increase in isometric force production with temperature in frog skeletal muscle. *J Physiol* 567, 459-469 (2005)

123. Coupland M.E. & K.W. Ranatunga: Force generation induced by rapid temperature jumps in intact mammalian (rat) skeletal muscle fibres. *J Physiol* 548, 439-449 (2003)

124. Bershitsky S.Y. & A.K. Tsaturyan: Effect of joule temperature jump on tension and stiffness of skinned rabbit muscle fibers. *Biophys J* 56, 809-816 (1989)

125. Bershitsky S.Y. & A.K. Tsaturyan: Tension responses to joule temperature jump in skinned rabbit muscle fibres. *J Physiol* 447, 425-448 (1992)

126. Kaplan J.H., B. Forbush 3rd & J.F. Hoffman: Rapid photolytic release of adenosine 5'-triphosphate from a protected analogue: utilization by the Na:K pump of human red blood cell ghosts. *Biochemistry* 17, 1929-1935 (1978)

127. Corrie J.E., A. Barth, V.R. Munasinghe, D.R. Trentham & M.C. Hutter: Photolytic cleavage of 1-(2-nitrophenyl)ethyl ethers involves two parallel pathways and product release is rate-limited by decomposition of a common hemiacetal intermediate. *J Am Chem Soc* 125, 8546-8554 (2003)

128. Barabás K. & L. Keszthelyi: Temperature dependence of ATP release from "caged" ATP. Acta Biochim Biophys Acad Sci Hung. 19, 305-309 (1984)

129. Goldman Y.E., M.G. Hibberd, J.A. McCray & D.R. Trentham: Relaxation of muscle fibres by photolysis of caged ATP. *Nature* 300, 701-705 (1982)

130. Goldman Y.E., M.G. Hibberd & D.R. Trentham: Relaxation of rabbit psoas muscle fibres from rigor by photochemical generation of adenosine-5'-triphosphate. *J Physiol* 354, 577-604 (1984)

131. Goldman Y.E., M.G. Hibberd & D.R. Trentham: Initiation of active contraction by photogeneration of adenosine-5'-triphosphate in rabbit psoas muscle fibres. *J Physiol* 354: 605-624 (1984)

132. Thirlwell H., J.E. Corrie, G.P. Reid, D.R. Trentham & M.A. Ferenczi: Kinetics of relaxation from rigor of permeabilized fast-twitch skeletal fibers from the rabbit using a novel caged ATP and apyrase. *Biophys J* 67, 2436-2447 (1994)

133. Poole K. J. V., G. Rapp, Y, Maeda & R.S. Goody: The time course of changes in equatorial diffraction patterns from different muscle types on photolysis of caged ATP. *Advances in Experimental Medicine and Biology* 226, 391-404 (1988)

134. Poole K. J. V., G. Rapp, Y. Maeda. & R.S. Goody: Structural transients in rabbit muscle after photolysis of caged ATP. *J Muscle Res Cell Motil* 8, 62 (1987)

135. Brenner B., M.A. Ferenczi, M. Irving, R.M. Simmons & E. Towns-Andrews: Myosin crossbridge movement observed by time-resolved X-ray diffraction in a single permeabilized fibre isolated from frog muscle. *J Physiol* 415, 113P (1989)

136. Horiuti K., N. Yagi & S. Takemori: Mechanical study of rat soleus muscle using caged ATP and X-ray diffraction: high ADP affinity of slow crossbridges. *J Physiol* 502, 433-447 (1997)

137. Yagi N., K. Horiuti & S. Takemori: A pre-active attached state of myosin heads in rat skeletal muscles. *J Muscle Res Cell Motil* 19, 75-86 (1998)

138. Horiuti K., N. Yagi, S. Takemori & M. Yamaguchi: An x-ray diffraction study on the ADP-induced conformational change in skeletal muscle myosin. *J Biochem (Tokyo)* 133, 207-210 (2003)

139. Takezawa Y., D.S. Kim, M. Ogino, Y. Sugimoto, T. Kobayashi, T. Arata & K. Wakabayashi: Backward movements of cross-bridges by application of stretch and by binding of MgADP to skeletal muscle fibers in the rigor state as studied by x-ray diffraction. *Biophys J* 76, 1770-1783 (1999)

140. Kaplan J.H. & G.C. Ellis-Davies: Photolabile chelators for the rapid photorelease of divalent cations. *Proc Natl Acad Sci U S A* 85, 6571-6575 (1988)

141. Brenner B., M.A. Ferenczi, M. Irving, J. Kaplan, R.M. Simmons & E. Towns-Andrews: Structural changes upon activation of single isolated muscle fibres of the frog by photolysis of 'caged-calcium' studied by time-resolved X-ray diffraction. *J Physiol* 418, 59P (1990)

142. Reedy M.K., K.C. Holmes & R.T. Tregear: Induced changes in orientation of the cross-bridges of glycerinated insect flight muscle. *Nature* 207, 1276-1280 (1965)

143. H.E. Huxley: The mechanism of muscular contraction. *Science* 164, 1356-1365 (1969)

144. Smith C.A. & I. Rayment: X-ray structure of the magnesium(II).ADP.vanadate complex of the Dictyostelium discoideum myosin motor domain to 1.9 A resolution. *Biochemistry* 35, 5404-5417 (1996)

145. Dominguez R., Y. Freyzon, K.M. Trybus & C. Cohen: Crystal structure of a vertebrate smooth muscle myosin motor domain and its complex with the essential light chain: visualization of the pre-power stroke state. *Cell* 94, 559-571 (1998)

146. Houdusse A., A.G. Szent-Gyorgyi & C. Cohen: Three conformational states of scallop myosin S1. *Proc Natl Acad Sci U S A* 97, 11238-11243 (2000)

147. Cooke R.: The mechanism of muscle contraction. *CRC Crit Rev Biochem* 21, 53-118 (1986)

148. Irving M., T. St Claire Allen, C. Sabido-David, J.S. Craik, B. Brandmeier, J. Kendrick-Jones, J.E. Corrie, D.R. Trentham & Y.E. Goldman: Tilting of the light-chain region of myosin during step length changes and active force generation in skeletal muscle. *Nature* 375, 688-691 (1995)

149. Hopkins S.C., C. Sabido-David, U.A. van der Heide, R.E. Ferguson, B.D. Brandmeier, R.E. Dale, J. Kendrick-Jones, J.E. Corrie, D.R. Trentham, M. Irving & Y.E. Goldman: Orientation changes of the myosin light chain domain during filament sliding in active and rigor muscle. *J Mol Biol* 318, 1275-1291 (2002)

150. Forkey J.N., M.E. Quinlan, M.A. Shaw, J.E. Corrie & Y.E. Goldman: Three-dimensional structural dynamics of myosin V by single-molecule fluorescence polarization. *Nature* 422, 399-404 (2003)

151. Uyeda T.Q., P.D. Abramson & J.A. Spudich: The neck region of the myosin motor domain acts as a lever arm to generate movement. *Proc Natl Acad Sci U S A* 93, 4459-4464 (1996)

152. Taylor K.A., H. Schmitz, M.C. Reedy, Y.E. Goldman, C. Franzini-Armstrong, H. Sasaki, R.T. Tregear, K. Poole, C. Lucaveche, R.J. Edwards, L.F. Chen., H. Winkler & M.K. Reedy: Tomographic 3D reconstruction of quick-frozen, Ca2+-activated contracting insect flight muscle. *Cell* 99, 421-431 (1999)

153. Reedy M.C.: Visualizing myosin's power stroke in muscle contraction. *J Cell Sci* 113, 3551-3562 (2000)

154. Molloy J.E., J. Kendrick-Jones, C. Veigel & R.T. Tregear: An unexpectedly large working stroke from chymotryptic fragments of myosin II. *FEBS Lett* 480, 293-297 (2000)

155. Huxley A.F.: Muscle structure and theories of contraction. *Prog Biophys Biophys Chem* 7, 255-318 (1957)

156. Holmes K.C., I. Angert, F.J. Kull, W. Jahn & R.R. Schroeder: Electron cryo-microscopy shows how strong binding of myosin to actin releases nucleotide. *Nature* 425, 423-427 (2003)

157. Berger C.L., J.S. Craik, D.R. Trentham, J.E. Corrie & Y.E. Goldman: Fluorescence polarization of skeletal muscle fibers labeled with rhodamine isomers on the myosin heavy chain. *Biophys J*. 71, 333033-43 (1996)

158. Poole K.J., M. Lorenz, G. Evans, G. Rosenbaum, A. Pirani, R. Craig, L.S. Tobacman, W. Lehman & K.C. Holmes: A comparison of muscle thin filament models obtained from electron microscopy reconstructions and low-angle X-ray fibre diagrams from non-overlap muscle. *J Struct Biol*. 155, 273-284 (2006)

159. Iwamoto H., J. Wakayama, T. Fujisawa & N. Yagi: Static and dynamic x-ray diffraction recordings from living

mammalian and amphibian skeletal muscles. *Biophys J*. 85, 2492-2506 (2003)

160. Ferenczi M.A., Y.E. Goldman & R.M. Simmons: The dependence of force and shortening velocity on substrate concentration in skinned muscle fibres from *Rana temporaria*. *J. Physiol*. 350, 519-543 (1984)

161. Cooke R., & E. Pate: The effects of ADP and phosphate on the contraction of muscle fibers. *Biophys J*. 48, 789-798 (1984)

162. Goldman Y.E. & R.M. Simmons: Control of sarcomere length in skinned muscle fibres of Rana temporaria during mechanical transients. *J Physiol*. 350, 497-518 (1984).

163. Pate E., G.J. Wilson, M. Bhimani & R. Cooke: Temperature dependence of the inhibitory effects of orthovanadate on shortening velocity in fast skeletal muscle. *Biophys J*. 66, 1554-1562 (1994)

164. Bershitsky S.Y. & A.K. Tsaturyan: Force generation and work production by covalently cross-linked actin-myosin cross-bridges in rabbit muscle fibers. *Biophys J*. 69, 1011-1021 (1995)

165. Tawada K., & M. Kimura: Stiffness of carbodiimide-crosslinked glycerinated muscle fibres in rigor and relaxing solutions at high salt concentrations. *J Muscle Res Cell Motil*. 7, 339-350 (1986)

166. Sutoh K.: Identification of myosin-binding sites on the actin sequence. *Biochemistry* 20, 3654-3661 (1982)

167. Grabarek Z. & J. Gergely: Zero-length crosslinking procedure with the use of active esters. *Anal Biochem*. 185, 131-135 (1990)

168. Furch M., B. Remmel, M.A. Geeves & D.J. Manstein: Stabilization of the actomyosin complex by negative charges on myosin. Biochemistry 39, 11602-11608 (2000)

169. Doyle T.C. & E. Reisler: Insights into actomyosin interactions from actin mutations. *Results Probl Cell Differ*. 36, 31-49 (2000)

170. Díaz Baños F.G., J. Bordas, J. Lowy & A. Svensson: Small segmental rearrangements in the myosin head can explain force generation in muscle. *Biophys J*. 71, 576-589 (1996)

Abbreviations and symbols: T_0: isometric tension; S1: myosin subfragment 1 or myosin head; CD: catalytic domain of S1; LCD: light chain domain of S1 or S1 'neck'; ATP: adenosine triphosphate; NPE-caged ATP: P^3-1-(2-nitrophenyl)ethyl ester of ATP; DMB-caged ATP: P^3-[1-(3,5-dimethoxyphenyl)-2-phenyl-2-oxo]ethyl ester of ATP; ADP: adenosine diphosphate; P_i: inorganic phosphate; EDC: 1-ethyl-3-[3-dimethylaminopropyl]-carbodiimide; A*X*: actin layer line with index *X*; M*X*: myosin layer line with index *X*; AM_{+1}, AM_{-1}: actin-myosin beating layer lines; I_Y: intensity of an x-ray reflection *Y*; Δ_{AR}, Δ_{MR}: radial deviations of the position of an actin (A) or a myosin (M) filament from its 'ideal' lattice point; *R*: radial coordinate in reciprocal space; *Z*: axial coordinate in reciprocal space

Key Words: Molecular Motor, Muscle Contraction, Myosin, Actin, X-Ray Diffraction, Review

Send correspondence to: Andrey K. Tsaturyan, Department of Biomechanics, Institute of Mechanics, Moscow University, 1 Mitchurinsky prosp. Moscow, 119992 Russia, Tel: 7 (495) 939 1252, Fax: 7 (495) 939 1252, E-mail: tsat@imec.msu.ru

http://www.bioscience.org/current/vol14.htm